

# Beyond Cross-Validation: Adaptive Parameter Selection for Kernel-Based Gradient Descents

**Xiaotong Liu**

*Center for Intelligent Decision-Making and Machine Learning,  
School of Management,  
Xi'an Jiaotong University, Xi'an, China*

ARIESOOMOON@GMAIL.COM

**Yunwen Lei**

*Department of Mathematics,  
The University of Hong Kong, Hongkong, China*

LEIYW@HKU.HK

**Xiangyu Chang**

**Shao-Bo Lin\***  
*Center for Intelligent Decision-Making and Machine Learning,  
School of Management,  
Xi'an Jiaotong University, Xi'an, China*

XIANGYUCHANG@GMAIL.COM

SBLIN1983@GMAIL.COM

**Editor:**

## Abstract

This paper proposes a novel parameter selection strategy for kernel-based gradient descent (KGD) algorithms, integrating bias–variance analysis with the splitting method. We introduce the concept of empirical effective dimension to quantify iteration increments in KGD, deriving an adaptive parameter selection strategy that is implementable. Theoretical verifications are provided within the framework of learning theory. Utilizing the recently developed integral operator approach, we rigorously demonstrate that KGD, equipped with the proposed adaptive parameter selection strategy, achieves the optimal generalization error bound and adapts effectively to different kernels, target functions, and error metrics. Consequently, this strategy showcases significant advantages over existing parameter selection methods for KGD.

**Keywords:** Parameter selection, nonparametric regression, gradient descent, kernel methods

## 1. Introduction

Parameter selection, often referred as hyperparameter selection, is a critical and longstanding research topic in statistics and machine learning. Selecting appropriate parameters in learning algorithms significantly impacts the accuracy, efficiency, and generalization capabilities of the resulting models. For instance, selecting suitable regularization parameters enables support vector machines (Steinwart and Christmann, 2008) to maintain a balance between bias and variance, ensuring excellent performance on unseen data, while tuning appropriate step sizes in stochastic gradient descent in deep learning (Bengio et al., 2017) succeeds in balancing the training time and model quality.

---

\*. Corresponding author

Parameter selection generally requires strategic approaches to ensure that the chosen parameters align with the specific goals and constraints of the learning task, triggering substantial research activity over the past two decades (Chapelle et al., 2002; De Vito et al., 2010; Caponnetto and Yao, 2010; Raskutti et al., 2014; Wei et al., 2019; Blanchard et al., 2019; Lu et al., 2020; Gizewski et al., 2022; Dinu et al., 2023; Lin, 2024). Broadly speaking, there are three basic ideas to parameter selection: the information entropy method, the splitting method, and the bias–variance analysis method. The information entropy method seeks to determine optimal parameters by balancing fitting accuracy with entropy-related complexity constraints and is particularly popular in linear methods (Reiss and Todd Ogden, 2009). Typical examples of the information entropy method include the Akaike information criterion (Akaike, 1974; Hurvich et al., 1998), the Bayesian information criterion (Schwarz, 1978; Mathias and Martyn, 2017), and the generalized information criterion (Nishii, 1984). The main advantage of this method is its ease of implementation, while a notable disadvantage is the difficulty in deriving provable generalization error bounds for non-linear algorithms. The splitting method focuses on selecting parameters by dividing the samples into a training set and a validation set, using the former to build models and the latter for parameter selection. Typical examples of this method include hold-out (Caponnetto and Yao, 2010), cross-validation (Györfi et al., 2002, Chap.8), and leave-one-out (Zhang, 2003). The advantages of the splitting method lie in its versatility, as it is applicable to nearly all learning algorithms, while the disadvantages stem from the exclusion of a portion of samples during the training process, which can lead to inflated generalization error. The bias–variance analysis method involves selecting parameters by balancing bias and variance, which are assessed using data-dependent and implementable quantities. Typical examples of this method include the balancing principle (Lu et al., 2020), the Lepskii principle (Blanchard et al., 2019), and the discrepancy principle (Celisse and Wahl, 2021). This method is advantageous for theoretical analysis but poses implementation challenges, as deriving precise bounds with optimal constants for bias and variance is quite difficult.

Due to its implementability, rapidity and versatility, the splitting method, especially cross-validation and hold-out, dominates in the modern statistics and machine learning. Statistical properties of hold-out, cross-validation and generalized cross-validation have been well developed by Caponnetto and Yao (2010), Xu et al. (2019), and Györfi et al. (2002, Chap.8), respectively. However, the splitting method frequently requires that the empirical excess risk is an accessible unbiased estimate of the population risk (Blanchard et al., 2019), making the corresponding parameter selection weak in tackling covariate shift problem in which the distributions of training and testing samples are different. Moreover, the commonly used truncation (or clip) operator that projects the derived estimates onto a finite interval (Györfi et al., 2002), not only makes parameter selection only available to bounded samples, but also deports the final models from the original hypothesis classes. The primary reason for these drawbacks is the lack of bias–variance analysis to highlight the detailed effects of parameters on bias and variance, which is crucial for addressing the covariate shift problem (Ma et al., 2023) and accessing unbounded samples (Blanchard and Krämer, 2016).

This paper aims to equip the classical splitting method with a delicate bias–variance analysis to circumvent the aforementioned drawbacks. Taking kernel-based gradient descent (KGD) (Lin and Zhou, 2018a; Yao et al., 2007) (also referred to as kernel-based boosting

in the literature (Raskutti et al., 2014; Wei et al., 2019)) as an example, we propose a novel hybrid selection scheme (HSS) that combines the hold-out (Caponnetto and Yao, 2010) and Lepskii-type principle (Blanchard et al., 2019; Lin, 2024) to adaptively determine the number of iterations for KGD with optimal theoretical verifications. According to the delicate bias–variance analysis, HSS first quantifies the bias of KGD by the increments between two successive iterations and the variance by the empirical effective dimension (Zhang, 2002). Then, taking the monotonicity of the involved quantities into account, it searches for the optimal number of iterations in a backward manner, i.e., from  $|D|$ ,  $|D| - 1$  to 1. In this way, a novel bias–variance analysis method with an unspecified constant independent of the data size is developed. HSS finally determines the constant by using the splitting method such as hold-out (or cross-validation) on a subset of samples. Under this circumstance, we obtain a parameter selection strategy that adapts to the kernels, target functions, and different metrics without discarding any samples.

Our main contributions can be concluded as follows. From the theoretical perspective, we prove that KGD equipped with the proposed HSS succeeds in achieving the optimal generalization error bounds established in (Lin and Zhou, 2018a), which demonstrates the effectiveness and optimality of HSS. This overcomes the bottlenecks of numerous parameter selection schemes such as the balancing principle (Lu et al., 2020) and discrepancy principle (Celisse and Wahl, 2021) that only lead to suboptimal generalization error bounds. Our main novelty in the proof is the introduction of several semi-adaptive stopping rules to quantify the range of the number of iterations determined by HSS. From the application perspective, the proposed HSS combines the bias–variance analysis and splitting methods to leverage their advantages in parameter selection and performs well in practice. We conduct both toy simulations and real data experiments to show the excellent performance of HSS, compared with hold-out (Caponnetto and Yao, 2010), Akaike information criterion (Akaike, 1974), Bayesian information criterion (Schwarz, 1978), balancing principle (Lu et al., 2020), Lepskii principle (Blanchard et al., 2019), early stopping rule (Raskutti et al., 2014), and discrepancy principle (Celisse and Wahl, 2021).

The rest of the paper is organized as follows. In the next section, we introduce HSS to equip KGD and compare our method with existing parameter selection strategies. Section 3 explores some important properties of HSS and derives the optimal generalization error bounds for KGD equipped with HSS. In Section 4, we conduct numerical experiments to demonstrate the feasibility of the proposed stopping rule. Section 5 provides further discussion. The proofs of our theoretical results are given in Appendix.

## 2. KGD with hybrid selection strategy

In this section, we introduce KGD with a hybrid selection strategy and compare it with some related works.

### 2.1 KGD with hybrid selection strategy

Let  $D = \{(x_i, y_i)\}_{i=1}^{|D|} \subset \mathcal{X} \times \mathcal{Y}$  be a sample set with  $|D|$  the cardinality of  $D$ ,  $\mathcal{X}$  a compact input space and  $\mathcal{Y} \subseteq \mathbb{R}$  an output space. Let  $K : \mathcal{X} \times \mathcal{X} \rightarrow \mathbb{R}$  be a Mercer kernel and  $\mathcal{H}_K$  be its corresponding reproducing kernel Hilbert space (RKHS) endowed with the inner

product  $\langle \cdot, \cdot \rangle_K$  and norm  $\| \cdot \|_K$ . Since  $\mathcal{X}$  is compact and  $K$  is a Mercer kernel, it is easy to check  $\kappa := \sqrt{\sup_{x \in \mathcal{X}} K(x, x)} < \infty$ . Kernel methods aim at finding a function  $f \in \mathcal{H}_K$  by minimizing the empirical risk

$$\mathcal{L}(f) := \frac{1}{|D|} \sum_{i=1}^{|D|} (y_i - f(x_i))^2. \quad (1)$$

The gradient of  $\mathcal{L}(f)$  with respect to  $f \in \mathcal{H}_K$  can be derived by Yao et al. (2007)

$$\nabla_f \mathcal{L}(f) = \frac{2}{|D|} \sum_{i=1}^{|D|} (f(x_i) - y_i) K_{x_i}. \quad (2)$$

Given a step size  $\beta > 0$ , KGD for (1) then can be formulated iteratively as

$$f_{t+1, \beta, D} = f_{t, \beta, D} - \frac{\beta}{|D|} \sum_{i=1}^{|D|} (f_{t, \beta, D}(x_i) - y_i) K_{x_i}, \quad (3)$$

where  $f_{0, \beta, D} = 0$  and  $K_{x_i}(\cdot) = K(x_i, \cdot)$ . It is obvious that  $f_{t, \beta, D} \in \mathcal{H}_K$  with the special format  $f_{t, \beta, D} = \sum_{i=1}^{|D|} c_i^t K_{x_i}$ . Let  $\mathbf{c}_t = (c_1^t, \dots, c_{|D|}^t)^\top$ ,  $y_D = (y_1, \dots, y_{|D|})^\top$  and  $\mathbb{K} = (K(x_i, x_{i'}))_{x_i, x_{i'} \in D}$  be the kernel matrix. It follows from (3) that

$$\mathbf{c}_{t+1} = \mathbf{c}_t - \frac{\beta}{|D|} (\mathbb{K} \mathbf{c}_t - y_D) \quad (4)$$

with  $\mathbf{c}_0 = (0, \dots, 0)^\top$ . Therefore, KGD requires  $\mathcal{O}(|D|^2)$  floating-point computations in each iteration. It was shown in (Lin and Zhou, 2018a; Yao et al., 2007) that KGD is an optimal learner in the sense of achieving the optimal generalization error bounds, provided the number of iterations is appropriately tuned. It has been widely used in regression (Yao et al., 2007), classification (Wei et al., 2019), minimum error entropy principle analysis (Hu et al., 2020) and testing (Hagrass et al., 2024).

As shown in Figure 1, the number of iterations,  $t$ , plays a crucial role in the sense that the best generalization performance of KGD is realized by setting the best  $t$  to balance the bias and variance. Our purpose is to propose a novel strategy to adaptively select  $t$  to approximate the best  $t$ . Our approach depends on a novel bias–variance analysis principle, called the backward selection principle (BSP), which is determined by the so-called empirical effective dimension of the kernel matrix (Zhang, 2002), defined by

$$\mathcal{N}_D(\lambda) := \text{Tr}[(\lambda |D| I + \mathbb{K})^{-1} \mathbb{K}], \quad \forall \lambda > 0, \quad (5)$$

where  $\text{Tr}$  denotes the trace of a matrix (or trace-class operator). Denote

$$\mathcal{W}_{D, t} := \left( \frac{\sqrt{t}}{|D|} + \frac{\sqrt{\max\{\mathcal{N}_D(t^{-1}), 1\}}(1 + \sqrt{t/|D|})}{\sqrt{|D|}} \right) \quad (6)$$

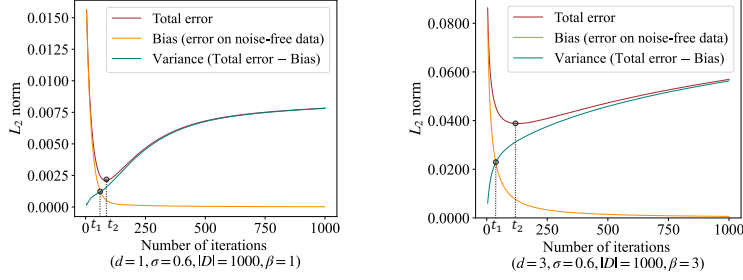


Figure 1: Role of the number of iterations in controlling the bias, variance and total error of KGD under the  $L_2$  norm. The training samples  $\{x_i\}_{i=1}^{1000}$  are independently drawn according to the uniform distribution on the (hyper-)cube  $[0, 1]^d$  with  $d = 1, 3$ . The corresponding outputs are generated by the model  $y_i = g_j(x_i) + \varepsilon_i, j = 1, 2$ , where  $g_1$  and  $g_2$  are defined by (43) and (44), respectively, and  $\varepsilon_i$  is the independent Gaussian noise  $\mathcal{N}(0, \sigma^2)$  with  $\sigma = 0.6$ . The bias and variance is defined by (23) below.

and

$$\mathcal{U}_{D,t,\delta} := \left( \frac{\log \left( 1 + 8 \log \frac{64}{\delta} \frac{\sqrt{t}}{\sqrt{|D|}} \max\{1, \mathcal{N}_D(t^{-1})\} \right)}{t^{-1}|D|} + \sqrt{\frac{\log \left( 1 + 8 \log \frac{64}{\delta} \frac{\sqrt{t}}{\sqrt{|D|}} \max\{1, \mathcal{N}_D(t^{-1})\} \right)}{t^{-1}|D|}} \right) \quad (7)$$

for any given  $\delta \in (0, 1)$ . Define further

$$T := T_{\delta,D} := \max_{1 \leq t \leq |D|} \{C_1^* \mathcal{U}_{D,t,\delta} \leq 1/2\} \quad (8)$$

with  $C_1^* := \max\{(\kappa^2 + 1)/3, 2\sqrt{\kappa^2 + 1}\}$ . Since  $\mathcal{U}_{D,t,\delta}$  increases with respect to  $t$ , the above  $T$  is well defined. We then define BSP for KGD as follows.

**Definition 1 (Backward Selection Principle (BSP))** *Given the confidence level  $\delta \in (0, 1)$  and the step size  $\beta$ , define  $\hat{t} := \hat{t}_{D,\beta} \in [1, T]$  as the largest integer satisfying*

$$t \|f_{t+1,\beta,D} - f_{t,\beta,D}\|_D + t^{1/2} \|f_{t+1,\beta,D} - f_{t,\beta,D}\|_K \geq \tilde{C} \mathcal{W}_{D,t} \log^2 \frac{16}{\delta}, \quad (9)$$

where  $\tilde{C}$  is a constant depending only on  $\kappa$  and the noise variance. If there is not any  $t \in [1, T]$  satisfying (9), we then set  $\hat{t} = T$ .

Figure 2 illustrates the feasibility of BSP in the sense that a given constant  $\tilde{C}$  follows a specific  $t_{\tilde{C}}$ . However, an excessively small or large  $\tilde{C}$  will directly lead to  $t_{\tilde{C}} = T$ . It is easy to check that the proposed BSP is a special type of Lepskii principle, with the only difference that the item-wise comparison in the classical principle (Blanchard et al., 2019; Lu et al.,

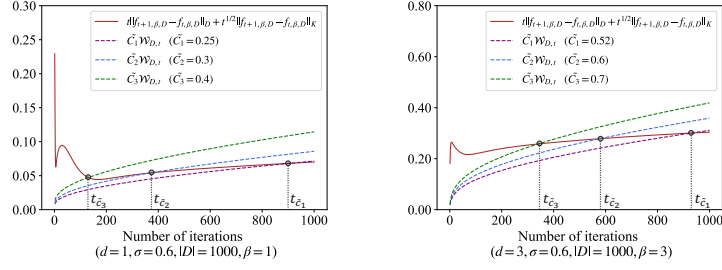


Figure 2: Step  $t_{\tilde{C}}$  determined by different values of the constant  $\tilde{C}$  under the BSP. The experimental setting is the same as in Figure 1.

2020) is removed. It should also be highlighted that BSP is not an early stopping scheme like that in (Raskutti et al., 2014), since BSP requires to run KGD from  $t = 1$  to  $t = T$  at first and then find the largest  $t$  satisfying (9). Due to (4), there are  $\mathbf{c}^{t+1} = (c_1^{t+1}, \dots, c_{|D|}^{t+1})^\top$  and  $\mathbf{c}^t = (c_1^t, \dots, c_{|D|}^t)^\top$  such that

$$f_{t+1, \beta, D} - f_{t, \beta, D} = \sum_{i=1}^{|D|} (c_i^{t+1} - c_i^t) K_{x_i}.$$

Then,

$$\|f_{t+1, \beta, D} - f_{t, \beta, D}\|_K^2 = \sum_{i=1}^{|D|} \sum_{j=1}^{|D|} (c_i^{t+1} - c_i^t)(c_j^{t+1} - c_j^t) K(x_i, x_j) = (\mathbf{c}^{t+1} - \mathbf{c}^t)^\top \mathbb{K} (\mathbf{c}^{t+1} - \mathbf{c}^t)$$

and

$$\|f_{t+1, \beta, D} - f_{t, \beta, D}\|_D^2 = \frac{1}{|D|} \sum_{i=1}^{|D|} (f_{t+1, \beta, D}(x_i) - f_{t, \beta, D}(x_i))^2 = \frac{1}{|D|} (\mathbf{c}^{t+1} - \mathbf{c}^t)^\top \mathbb{K}^2 (\mathbf{c}^{t+1} - \mathbf{c}^t),$$

which together with (5) and (6) makes the BSP in Definition 1 implementable.

Due to (6), the parameter selection strategy requires to compute the effective dimension  $\mathcal{N}_D(t^{-1}) = \text{Tr}[(t^{-1}|D|I + \mathbb{K})^{-1}\mathbb{K}]$  for different  $t$ . Noting that the eigenvectors for the matrices  $\mathbb{K}$  and  $(t^{-1}|D|I + \mathbb{K})^{-1}$  are the same, if the eigenvalues of  $\mathbb{K}$ , denoted by  $\{\sigma_1^x, \dots, \sigma_{|D|}^x\}$  in a decreasing order, are obtained, then the empirical effective dimension for any  $t$  can be obtained by  $\mathcal{N}_D(t^{-1}) = \sum_{i=1}^{|D|} \frac{\sigma_i^x}{\sigma_i^x + t^{-1}|D|}$ . Hence, BSP requires to compute eigenvalues of  $\mathbb{K}$  and needs  $\mathcal{O}(|D|^3)$ , which is similar to that in the early stopping rule proposed in (Raskutti et al., 2014), although early stopping in (Raskutti et al., 2014) forces termination of the iteration before  $t = |D|$ .

In implementing BSP, we need to determine the constants  $\kappa$ ,  $M$  and the confidence level  $\delta$ . It is well known that estimating the noise variance  $M$  is not easy, but we can utilize the approach in (Raskutti et al., 2014) to approximately compute it, which makes BSP numerically feasible. The main problem is that the derived constant  $\tilde{C}$  in (9) is generally not optimal, leading BSP to be far from optimal. Fortunately, we find that the constant, as

---

**Algorithm 1** KGD with HSS
 

---

**Inputs:**  $D = \{(x_i, y_i)\}_{i=1}^m$ , set of constants  $\mathcal{C}_U := \{\hat{C}_j\}_{j=1}^U$  with  $U \in \mathbb{N}$ , step size  $0 < \beta \leq \frac{1}{\kappa}$  and the kernel  $K$ .

**Data Split:** For  $L \leq |D|$ , select  $L$  samples from  $D$  randomly according to the uniform distribution. Divide the selected samples into the training set  $D_{tr,L}$  and validation set  $D_{val,L}$ .

**Compute the empirical effective dimension:** Compute eigenvalues of two kernel matrices  $\mathbb{K} = (K(x_i, x_{i'}))_{x_i, x_{i'} \in D}$  and  $\mathbb{K}_L = (K(x_i, x_{i'}))_{x_i, x_{i'} \in D_{tr,L}}$  and denote them by  $\{\sigma_i^x\}_{i=1}^{|D|}$  and  $\{\sigma_{i,L}^x\}_{i=1}^{|D|}$ , respectively. Compute  $\mathcal{W}_{D,t}$  and  $\mathcal{W}_{D_{tr,L},t}$  via (5) and (6) for  $t = 1, \dots, |D|$ .

**Compute the sudden stopping value  $T$ :** Given a confidence level  $\delta \in (0, 1)$ , compute  $\mathcal{U}_{D,t,\delta}$  according to (7) and then determine  $T$  via (8).

**KGD:** Set  $f_{0,\beta,D} = 0$  and  $f_{0,\beta,D_{tr,L}} = 0$ . Obtain two sequences of KGD estimators  $\{f_{t+1,\beta,D}\}_{t=0}^{|D|-1}$  and  $\{f_{t+1,\beta,D_{tr,L}}\}_{t=0}^{|D|-1}$  via (3).

**Selecting the constant:** Define  $\hat{t}_j \in [1, T]$  to be the largest integer satisfying

$$t \|f_{t+1,\beta,D_{tr,L}} - f_{t,\beta,D_{tr,L}}\|_{D_{tr,L}} + t^{1/2} \|f_{t+1,\beta,D_{tr,L}} - f_{t,\beta,D_{tr,L}}\|_K \geq \hat{C}_j \mathcal{W}_{D_{tr,L},t}. \quad (10)$$

If (10) does not hold for all  $t \in [1, T]$ , set  $\hat{t}_j = T$ . Define

$$j^* := \arg \min_{j=1,\dots,U} \frac{1}{|D_{val,L}|} \sum_{(x,y) \in D_{val,L}} (f_{\hat{t}_j,\beta,D_{tr,L}}(x) - y)^2. \quad (11)$$

**BSP for final parameter:** Define  $\hat{t}^* \in [1, |D|]$  to be the largest integer satisfying

$$t \|f_{t+1,\beta,D} - f_{t,\beta,D}\|_D + t^{1/2} \|f_{t+1,\beta,D} - f_{t,\beta,D}\|_K \geq \hat{C}_{j^*} \mathcal{W}_{D,t}. \quad (12)$$

**Output:**  $f_{\hat{t}^*,\beta,D}$ .

---

well as the confidence level  $\delta$  that could be specified before the learning process to reflect the user's confidence, are independent of the data size. Therefore, we can use the hold-out or cross-validation approaches to select it by running KGD with BSP on a small dataset, for example, drawing  $|D|/10$  samples from  $D$ . In this way, we actually obtain an adaptive parameter selection strategy by combining BSP with cross-validation. We name this novel strategy the hybrid selection strategy (HSS), as shown in Algorithm 1.

We then present several comments on Algorithm 1 as follows.

◇ **Constant candidates:** HSS should quantify the set  $\mathcal{C}_U$  before the training. Recalling (9), we note that  $\mathcal{C}_U$  possesses an upper bound  $4(1+\beta)\tilde{C} \log^4 \frac{16}{\delta}$ . A favorable setting is to set  $\mathcal{C}_U = \{4(1+\beta)\tilde{C} \log^4 \frac{16}{\delta} q^k : k = 0, 1, \dots, \}$  for some  $0 < q < 1$ . The problem is, however, that  $4(1+\beta)\tilde{C} \log^4 \frac{16}{\delta}$  itself is not easy to compute, since it requires to obtain the noise of the data. Numerically, we can set

$$\mathcal{C}_U := \left\{ \tilde{C}_0 q^k : k = 0, 1, \dots, U \right\} \quad (13)$$

for a sufficiently large  $\tilde{C}_0$ , i.e.,  $\tilde{C}_0 = 100$ ,  $q = 9/10$  and  $U = 20$  for example.

◇ **Computation reduction:** since the constant  $4(1+\beta)\tilde{C} \log^4 \frac{16}{\delta}$  in (9) is independent of the data and the selection of  $L \leq |D|$  samples in the parameter selection strategy is only for selecting a suitable constant to feed BSP, the subsampling scheme in the data split step does not affect the selection of the final constants in theory. In computing the empirical effective

dimension step, it is not necessary to compute all  $\mathcal{W}_{D,t}$  and  $\mathcal{W}_{D_{tr,L},t}$ . Indeed, we can select  $t$  backward from  $|D|$  to 1 and stop the search once (10) and (12) are satisfied. Under this circumstance, we only need to compute  $\mathcal{W}_{D,t}$  and  $\mathcal{W}_{D_{tr,L},t}$  for  $t$  not smaller than the value determined by (10) and (12). Recalling that  $\mathcal{N}_D(t^{-1}) = \sum_{i=1}^{|D|} \frac{\sigma_i^x}{\sigma_i^x + t^{-1}|D|}$ , computing  $\mathcal{W}_{D,t}$  and  $\mathcal{W}_{D_{tr,L},t}$  for all  $t$  does not incur much additional computation, we suggest computing all of them in the algorithm. Once the constant  $C_j^*$  is determined, we then use the whole sample to derive a final parameter  $\hat{t}^*$  to feed KGD. If we set  $L \leq |D|/U^{1/3}$ , it is easy to check that there are totally  $\mathcal{O}(|D|^3)$  floating-point computations in implementing KGD with HSS.

◇ **Early-stopping and BSP:** Different from (Raskutti et al., 2014) that equips KGD with an early stopping scheme, our proposed strategy in Algorithm 1 requires to run KGD over all  $t \in [1, T]$ . However, it should be highlighted that all existing early-stopping parameter selection strategies (Raskutti et al., 2014; Wei et al., 2019) require to compute the eigenvalues of  $\sigma_i^x$  for  $i = 1, \dots, |D|$ , needing  $\mathcal{O}(|D|^3)$  computational complexity. Under this circumstance, whether an early stopping parameter selection strategy is employed does not affect the computational complexity essentially. Our proposed HSS strategy, compared with those in (Raskutti et al., 2014; Wei et al., 2019), dominates in reflecting the regularity of data precisely.

◇ **Lepskii principle versus discrepancy principle:** Lepskii and discrepancy principles are two popular principles used to design parameter selection strategy for kernel methods (De Vito et al., 2010; Lu et al., 2020; Blanchard et al., 2019; Celisse and Wahl, 2021; Lin, 2024). The former focuses on selecting parameters by bounding differences of two successive estimates while the latter is devoted to quantifying the fitting error by some computable quantities. They are essentially different approaches for general kernel methods (Blanchard et al., 2019; Celisse and Wahl, 2021). However, due to the special spectral property of KGD (Lin and Zhou, 2018a), i.e.,  $f_{t+1,\beta,D} - f_{t,\beta,D} = \beta (L_{K,D} f_{t,\beta,D} - S_D^\top y_D)$ , Lepskii and discrepancy principles are the same for KGD. That is, the philosophy behind HSS is both the Lepskii principle and discrepancy principle.

## 2.2 Related works

In this part, we compare the proposed adaptive stopping rule with some related works. KGD was initially studied in (Yao et al., 2007; Gerfo et al., 2008) as a special class of kernel-based spectral algorithms to conquer the saturation of kernel ridge regression (Caponnetto and De Vito, 2007). Optimal generalization error bounds of KGD were established in (Yao et al., 2007; Raskutti et al., 2014; Lin and Zhou, 2018a) under different assumptions on data and kernels. However, all these optimal generalization error bounds were established on the condition that the number of iterations is appropriately selected. Although several stopping rules including the discrepancy principle (Engl et al., 1996, Chap.6) and balancing principle (Lazarov et al., 2007) have been proposed to determine the number of iterations in the framework of inverse problems, it is highly non-trivial to develop stopping rules for KGD in the nonparametric regression community. In the following, we introduce existing strategies to select the number of iterations for KGD.

- Baseline (BS): The number of iterations is determined by

$$t_{BS} := \arg \min_{t \in [0, |D|]} \|f_{t, \beta, D} - f_\rho\|_D^2. \quad (14)$$

The baseline defined by (14) is a theoretically optimal parameter selection strategy to determine  $t$  in KGD under the assumption that the exact knowledge of the target function  $f_\rho$  is known. It numerically performs well but requires the access of  $f_\rho$ , which is practically infeasible. We introduce this method only to provide a reference to judge the quality of other implementable parameter selection strategies.

- Hold-out (HO): The number of iterations is determined by

$$t_{HO} := \arg \min_{t \in [0, |D|]} M_{HO}(f_{t, \beta, D_{tr}}). \quad (15)$$

To be detailed, the hold-out (or cross-validation CV) (Caponnetto and Yao, 2010; Lin and Zhou, 2018b; Zhang, 2003) method is a numerically feasible method for selecting  $t$  from  $[0, |D|]$  to achieve optimal generalization error bounds of KGD. It requires splitting the sample set  $D$  into training and validation sets, denoted as  $D_{tr}$  and  $D_{val}$ , respectively, where  $D = D_{tr} \cup D_{val}$ ,  $D_{tr} \cap D_{val} = \emptyset$  and  $D_{tr}$  contains half of the whole sample data. It then evaluates the performance of KGD on  $D_{val}$  via  $M_{HO}(f_{t, \beta, D_{tr}}) := \frac{1}{|D_{val}|} \sum_{(x_i, y_i) \in D_{val}} (y_i - f_{t, \beta, D_{tr}}(x_i))^2$  and selects  $t$  to minimize the validation error. The optimality of HO for KGD can be easily derived by using the same method as in (Lin and Zhou, 2018b). The problem is, however, that the split of samples reduces the numerical performance of KGD itself.

- Balancing principle (BP): Given the confidence level  $\delta$ , the number of iterations is determined by

$$t_{BP} := \min \left\{ t \in [0, |D|] : \|f_{t', \beta, D} - f_{t, \beta, D}\|_D \leq C_{BP} \mathcal{W}_{D, t'} \log^4 \frac{16}{\delta}, t' = t + 1, \dots, |D| \right\}, \quad (16)$$

where  $\mathcal{W}_{D, t}$  is defined by (6) and  $C_{BP} > 0$  is a constant independent of  $|D|$ ,  $\delta$  or  $t$ . The balancing principle was initially proposed in (De Vito et al., 2010) in the framework of learning theory to select a regularization parameter for KRR and then developed in (Lu et al., 2020) for determining parameters of kernel-based spectral algorithms. It can be found in (16) that the balancing principle does not require a split of the sample set.

- Lepskii principle (LP): Given  $q > 1$  and  $0 < \delta < 1$ , define  $T_q := \{t_i = q^i / (\kappa^2) : i \in \mathbb{N}\}$ ,  $L_{\delta, q} = 2 \log \left( \frac{8 \log |D|}{\delta \log q} \right)$  and  $T_{\mathbf{x}} := \left\{ t \in T_q : t \leq \max \left\{ \frac{|D|}{100 \kappa^2 L_{\delta, q}^2}, \frac{|D|}{3 \kappa^2 (\mathcal{N}_D(t^{-1}) + 1)} \right\} \right\}$ . The number of iterations is determined by

$$t_{LP} := \min \left\{ t \in T_{\mathbf{x}} : \|(L_{K, D} + t'^{-1} I)^{1/2} (f_{t', \beta, D} - f_{t, \beta, D})\|_K \leq C_{LP} \mathcal{W}_{D, t'}^*, t' \geq t, t' \in T_{\mathbf{x}} \right\}. \quad (17)$$

where  $\mathcal{W}_{D, t}^* = \frac{\sqrt{t(\mathcal{N}_D(t^{-1}) + 1)}}{\sqrt{|D|}}$ . The Lepskii principle was first proposed in (Blanchard et al., 2019) to improve the performance of balancing principle in supervised learning. The oracle property of the Lepskii principle was verified in (Blanchard et al., 2019). In particular, it can be found in (Blanchard et al., 2019) that KGD equipped with the Lepskii principle can achieve the almost optimal generalization error bounds. Similar to BP, LP also needs item-wise comparisons for a given constant  $C_{LP}$ . Since  $C_{LP}$  is practically unknown, it frequently requires heavy computation.

- Early stopping rule (ESR): Define the local empirical Rademacher complexity of the kernel matrix  $\mathbb{K}$  to be  $\hat{\mathcal{R}}_{\mathbb{K}}(\epsilon) := \left[ \frac{1}{|D|} \sum_i \min\{\sigma_i^x, \epsilon^2\} \right]^{1/2}$ . Denote  $\eta_t = t\beta$ . Let  $t_{ESR}$  be the first positive number satisfying

$$\hat{\mathcal{R}}_{\mathbb{K}}(1/\sqrt{\eta_t}) > C_{ESR}(\tau\eta_t)^{-1}, \quad (18)$$

where  $\tau > 0$  is the standard deviation of noise and can be estimated by the classical method in (Hall and Marron, 1990), and  $C_{ESR} > 0$  is a tuning parameter, suggested to be  $2e$  by Raskutti et al. (2014). The work in (Raskutti et al., 2014) is the first result, to the best of our knowledge, that designs an exclusive early stopping rule for KGD with theoretical guarantees. Different from the above four methods, ESR does not require to run KGD over  $[1, |D|]$ . The problem is, however, that such an early stopping rule is not adaptive to the regularity of the target function in the sense that it only holds under the assumption that the target function is in  $\mathcal{H}_K$ .

- Discrepancy principle (DP): Given a noise level  $\sigma^2$ , the discrepancy principle, which is a classical and widely used strategy to select parameters in inverse problems, is defined by Engl et al. (1996, Sec.4.3),

$$t_{DP} := \inf_{t \in [1, |D|]} \{\|y_D - S_D f_{t, \beta, D}\|_{\ell^2} \leq C_{DP} \sigma^2\},$$

where  $C_{DP}$  is a constant independent of  $t$  or  $|D|$ . However, it is non-trivial to quantify the noise level  $\sigma^2$  for supervised learning, which hinders the usage of DP. The interesting work (Celisse and Wahl, 2021) modified the discrepancy principle for the learning purpose by introducing the computation of the noise level and an emergency stop rule. Theoretical analysis has also been conducted in (Celisse and Wahl, 2021) to verify the effectiveness of the discrepancy principle in the framework of learning theory. The problem is, however, that the derived generalization error bounds are suboptimal (Celisse and Wahl, 2021, Theorem 20).

- Akaike information criterion (AIC): Let  $\mathcal{W}_{D,t}$  be defined by (6) to mimic the degree of freedom in the kernel learning framework. AIC, introduced by Akaike (1974) for linear methods, aims to introduce an additional penalty to balance the fitting accuracy and model complexity and can be mathematically defined by

$$t_{AIC} := \inf_{t \in [1, |D|]} \|y_D - S_D f_{t, \beta, D}\|_{\ell^2} + C_{AIC} \mathcal{W}_{D,t}.$$

Although the defined penalty in the above definition is slightly different from that in (Demjanov et al., 2012), the main idea remains the same, i.e., using some implementable quantities to measure the degree of freedom to act as the penalty. Some statistical properties of this type of AIC have been investigated in (Claeskens et al., 2008), but deriving provable generalization error bounds for the corresponding algorithms remains challenging. In this case, we cannot theoretically verify the adaptivity of the defined AIC.

- Bayesian information criterion (BIC): BIC was originally introduced by Schwarz (1978) for linear methods and can be extended to KGD via

$$t_{BIC} := \inf_{t \in [1, |D|]} \|y_D - S_D f_{t, \beta, D}\|_{\ell^2} + C_{BIC} \mathcal{W}_{D,t} \log |D|.$$

Compared with AIC, BIC includes an additional  $\log|D|$  term in the penalty, and its statistical properties, similar to those of AIC, have been discussed in (Demianov et al., 2012). Mathematically, it is easy to derive that  $t_{BIC} \leq t_{AIC}$ . However, similar to AIC, it is also difficult to theoretically verify the adaptivity of BIC in terms of deriving optimal generalization error bounds for the corresponding KGD.

### 3. Theoretical behaviors

In this section, we present theoretical verifications of the proposed HSS for KGD.

#### 3.1 Bias and variance analysis of KGD

We conduct the bias–variance analysis of KGD in the framework of nonparametric regression (Györfi et al., 2002), in which the samples  $\{(x_i, y_i)\}_{i=1}^{|D|}$  are assumed to be independently and identically drawn from an unknown distribution  $\rho := \rho_X \times \rho(y|x)$  with  $\rho_X$  the marginal distribution and  $\rho(y|x)$  the conditional distribution on  $x$ . The aim of learning is to find an estimator to approximate the regression function  $f_\rho = \int_{\mathcal{Y}} y d\rho(y|x)$ , which minimizes the generalization error  $\mathcal{E}(f) := \int (f(x) - y)^2 d\rho$ . Let  $L_{\rho_X}^2$  denote the space of  $\rho$ -square integrable functions endowed with norm  $\|\cdot\|_\rho$ . It is easy to check

$$\mathcal{E}(f) - \mathcal{E}(f_\rho) = \|f - f_\rho\|_\rho^2, \quad f \in L_{\rho_X}^2. \quad (19)$$

The learning performance of KGD has been extensively studied in (Yao et al., 2007; Raskutti et al., 2014; Lin and Zhou, 2018a) under assumptions on noise, regularity of the regression function, and capacity of the kernel.

**Assumption 1 (Noise assumption:)** Assume  $\int_{\mathcal{Y}} y^2 d\rho < \infty$  and

$$\int_{\mathcal{Y}} \left( e^{\frac{|y - f_\rho(x)|}{M}} - \frac{|y - f_\rho(x)|}{M} - 1 \right) d\rho(y|x) \leq \frac{\gamma^2}{2M^2}, \quad \forall x \in X, \quad (20)$$

where  $M$  and  $\gamma$  are positive constants.

Condition (20) is the standard Bernstein assumption on the noise (Caponnetto and De Vito, 2007; Blanchard and Krämer, 2016), which can be satisfied when the noise is uniformly bounded, Gaussian or sub-Gaussian. To introduce the regularity assumption, we define the following positive operator  $L_K : \mathcal{H}_K \rightarrow \mathcal{H}_K$  (or  $L_{\rho_X}^2 \rightarrow L_{\rho_X}^2$  when there is no ambiguity) as  $L_K(f) := \int_X f(x) K_x d\rho_X$ . The positivity is guaranteed since  $K$  is a Mercer kernel.

**Assumption 2 (Regularity assumption:)** There exists an  $r > 0$  such that

$$f_\rho = L_K^r(h_\rho), \quad h_\rho \in L_{\rho_X}^2, \quad r > 0, \quad (21)$$

where  $L_K^r$  is the  $r$ -th power of  $L_K$ .

Assumption 2 has been widely used in literature (Caponnetto and De Vito, 2007; Yao et al., 2007; Blanchard and Krämer, 2016; Guo et al., 2017; Lin et al., 2017) and the exponent  $r$  quantifies the regularity of  $f_\rho$ . It should be noted that (21) with  $r = 1/2$  implies  $f_\rho \in \mathcal{H}_K$  and vice versa (Caponnetto and De Vito, 2007). Moreover, a larger  $r$  indicates better regularity of the regression functions.

We then study the role of iterations in the learning process from the bias and variance perspective to pursue the selection of optimal  $t$  for KGD. Let  $f_{t,\beta,D}^\diamond := E[f_{t,\beta,D}|x]$  be the noise-free version of  $f_{t,\beta,D}$ . It follows from (3) that

$$f_{t+1,\beta,D}^\diamond = f_{t,\beta,D}^\diamond - \frac{\beta}{|D|} \sum_{i=1}^{|D|} (f_{t,\beta,D}^\diamond(x_i) - f_\rho(x_i)) K_{x_i}. \quad (22)$$

Then, the triangle inequality yields

$$\|f_{t+1,\beta,D} - f_\rho\|_\rho \leq \overbrace{\|f_{t+1,\beta,D}^\diamond - f_\rho\|_\rho}^{\text{Bias}} + \overbrace{\|f_{t+1,\beta,D}^\diamond - f_{t+1,\beta,D}\|_\rho}^{\text{Variance}}. \quad (23)$$

The following lemma which can be found in (Lu et al., 2020; Lin et al., 2019) establishes a relation between  $\|f\|_\rho$ ,  $\|f\|_D$  and  $\|f\|_K$ .

**Lemma 1** *Let  $f \in \mathcal{H}_K$ . Then*

$$\|f\|_\rho \leq \mathcal{Q}_{D,t}(\|f\|_D + t^{-1/2}\|f\|_K), \quad (24)$$

where

$$\mathcal{Q}_{D,t} := \|(L_{K,D} + t^{-1}I)^{-1/2}(L_K + t^{-1}I)^{1/2}\| \quad (25)$$

and  $\|A\|$  denotes the spectral norm of the operator  $A$ .

Due to the above lemma, to study the role of  $t$  in bounding  $\|f_{t,\beta,D} - f_\rho\|_\rho$ , it suffices to analyze its effect on  $\|f_{t,\beta,D} - f_\rho\|_D + t^{-1/2}\|f_{t,\beta,D} - f_\rho\|_K$ . From (23), the bias and variance can be bounded by

$$\mathcal{B}_{t,\beta,D} := \|f_{t,\beta,D}^\diamond - f_\rho\|_D + t^{-1/2}\|f_{t,\beta,D}^\diamond - f_\rho\|_K \quad (26)$$

and

$$\mathcal{V}_{t,\beta,D} := \|f_{t,\beta,D}^\diamond - f_{t,\beta,D}\|_D + t^{-1/2}\|f_{t,\beta,D}^\diamond - f_{t,\beta,D}\|_K. \quad (27)$$

The following proposition illustrates how  $t$  controls the bias and variance via (6) and the effective dimension  $\mathcal{N}(\lambda)$  (Zhang, 2002) defined by  $\mathcal{N}(\lambda) := \text{Tr}[(\lambda I + L_K)^{-1}L_K]$  with  $\lambda > 0$ .

**Proposition 2** *Let  $0 < \delta < 1$ ,  $f_{t,\beta,D}$  and  $f_{t,\beta,D}^\diamond$  be defined by (3) and (22) with  $t \leq T$  and  $0 < \beta \leq \kappa^{-1}$ . Under Assumption 1 and Assumption 2 with  $r \geq 1/2$ , with confidence  $1 - \delta$ , there hold*

$$\mathcal{B}_{t,\beta,D} \leq \log^2 \frac{16}{\delta} \begin{cases} 2^{r-\frac{1}{2}} t^{-r}, & \text{if } \frac{1}{2} \leq r \leq 1, \\ t^{-r} + 4\kappa^2 t^{-\frac{1}{2}} |D|^{-\min\{1/2, (r/2-1/4)\}}, & \text{if } r > 1 \end{cases} \quad (28)$$

and

$$\mathcal{V}_{t,\beta,D} \leq 2\sqrt{2}(\kappa M + \gamma)(1 + \beta)\mathcal{A}_{D,\lambda} \log \frac{8}{\delta} \leq 2(1 + \beta)\mathcal{W}_{D,t} \log^2 \frac{16}{\delta}, \quad (29)$$

where

$$\mathcal{A}_{D,t} := \frac{1}{\sqrt{|D|}} \left( \frac{\sqrt{t}}{\sqrt{|D|}} + \sqrt{\mathcal{N}(t^{-1})} \right). \quad (30)$$

Proposition 2 presents the trends of bias and variance as the number of iterations  $t$  changes. It can be found in (6) and (29) that the upper bound of variance increases with the number of iterations. On the contrary, (28) shows that the upper bound of bias is monotonically decreasing with respect to  $t$ . Therefore, there exists an optimal  $t$  minimizing the generalization error of KGD. Let  $\{(\sigma_\ell, \varphi_\ell)\}_\ell$  be a set of normalized eigenpairs of  $L_K$  on  $\mathcal{H}_K$  with  $\{\varphi_\ell\}_\ell$  being an orthonormal basis of  $\mathcal{H}_K$  and  $\{\sigma_\ell\}_\ell$  arranged in a non-increasing order. Based on Proposition 2, we can derive the following corollary to show the generalization error bounds for KGD with appropriately tuned parameter  $t$  under different decaying rates of  $\sigma_\ell$ .

**Corollary 3** *Let  $0 < \delta < 1$ ,  $f_{t,\beta,D}$  be defined by (3) with  $t \leq T$  and  $0 < \beta \leq \kappa^{-1}$ . Under Assumption 1 and Assumption 2 with  $r \geq 1/2$ , if*

$$t \sim \begin{cases} (|D|/L)^{\frac{1}{2r}}, & \text{if } \sigma_\ell = 0, \ell \geq L + 1, \\ |D|^{\frac{1}{2r+s}}, & \text{if } \sigma_\ell \leq c_0 \ell^{-1/s}, \\ (|D|/\sqrt{\log |D|})^{\frac{1}{2r}}, & \text{if } \sigma_\ell \leq c_1 e^{-c_2 \ell^2}, \end{cases} \quad (31)$$

then with confidence  $1 - \delta$ , there holds

$$\begin{aligned} & \max\{\|f_{D,t} - f_\rho\|_\rho, \|f_{D,t} - f_\rho\|_D, t^{1/2}\|f_{D,t} - f_\rho\|_K\} \\ & \leq \tilde{C} \log^2 \frac{16}{\delta} \begin{cases} (|D|/L)^{-1/2}, & \text{if } \sigma_\ell = 0, \ell \geq L + 1, \\ |D|^{-r/(2r+s)}, & \text{if } \sigma_\ell \leq c_0 \ell^{-1/s}, \\ (|D|/\sqrt{\log |D|})^{-1/2}, & \text{if } \sigma_\ell \leq c_1 e^{-c_2 \ell^2}, \end{cases} \end{aligned} \quad (32)$$

where  $\tilde{C}$  is a constant independent of  $\delta$ ,  $|D|$ , or  $t$ .

It can be found in (Caponnetto and De Vito, 2007; Raskutti et al., 2012) that the established generalization error bound for KGD is optimal in the minimax sense, and the learning performance of KGD is independent of the step size  $\beta$ , provided  $0 < \beta \leq \kappa^{-1}$ . The aforementioned theoretical verification indicates the superiority of KGD, but selecting an appropriate parameter  $t$  to optimize its learning capability remains open since the theoretically optimal parameter  $t_0$  satisfying (31) cannot be directly obtained in practice. From (31), we find that the theoretically optimal  $t$  for the finite rank and exponential decaying  $L_K$  is independent of  $s$ . Hence, if the kernel and  $\rho_X$  are specified to make  $L_K$  be finite rank or exponential decaying, it is not necessary to make the stopping rule adaptive to kernels. Recalling (32), the generalization error bounds under the  $\|\cdot\|_\rho$  norm for finite rank and exponential decaying  $L_K$  are independent of  $r$ . However, for the  $\mathcal{H}_K$  norm, the index  $r$  is crucial. For example, if  $L_K$  is of finite rank  $L$ , then we can derive from (32) that  $\|f_{D,t} - f_\rho\|_K \leq \tilde{C} \left(\frac{L}{|D|}\right)^{\frac{1-1/2r}{2}} \log^2 \frac{16}{\delta}$ , which has not been considered in (Raskutti et al., 2014; Zhang et al., 2015) as only  $r = 1/2$  is analyzed.

Since the computation of bias and variance in Proposition 2 requires access to the regression function that is unknown in practice, we adopt an alternative approach by leveraging the iterative nature of KGD. Our basic idea is to control the error increments of successive iterations in the following proposition.

**Proposition 4** *Let  $0 < \delta < 1$  and  $f_{t,\beta,D}$  be defined by (3) with  $t \in \mathbb{N}$  and  $0 < \beta \leq \kappa^{-1}$ . Under Assumption 1 and Assumption 2 with  $r \geq 1/2$ , with confidence  $1 - \delta$ , there holds*

$$\begin{aligned} & \|f_{t+1,\beta,D} - f_{t,\beta,D}\|_D + t^{-1/2} \|f_{t+1,\beta,D} - f_{t,\beta,D}\|_K \\ & \leq 2\sqrt{2} \log^2 \frac{16}{\delta} (\beta + 1) t^{-1} \mathcal{W}_{D,t} + C'_1 \log^2 \frac{16}{\delta} \begin{cases} 2^{r-1/2} t^{-r-1}, & \text{if } \frac{1}{2} \leq r \leq 1, \\ t^{-r-1} + 4\kappa^2 t^{-3/2} |D|^{-\min\{1/2, r/2-1/4\}}, & \text{if } r > 1, \end{cases} \end{aligned} \quad (33)$$

where  $C'_1$  is a constant independent of  $|D|$ ,  $t$  or  $\delta$ .

Comparing Proposition 4 with Proposition 2, we find that  $t\|f_{t+1,\beta,D} - f_{t,\beta,D}\|_D + t^{1/2}\|f_{t+1,\beta,D} - f_{t,\beta,D}\|_K$  behaves the same as  $\mathcal{V}_{t,\beta,D} + \mathcal{B}_{t,\beta,D}$  with respect to  $t$ . The only difference is that  $\|f_{t+1,\beta,D} - f_{t,\beta,D}\|_D$  and  $\|f_{t+1,\beta,D} - f_{t,\beta,D}\|_K$  are numerically realizable but  $\|f_{t,\beta,D} - f_\rho\|_D$  or  $\|f_{t,\beta,D} - f_\rho\|_K$  is incomputable. Therefore, it is possible to quantify the increments of successive iterations to develop a parameter selection strategy like (9) to yield perfect theoretical results of the generalization error  $\|f_{t,\beta,D} - f_\rho\|_\rho$ .

### 3.2 Semi-adaptive stopping rules and upper bound of iterations

To study the property of HSS, especially the upper bound of  $\hat{t}$ , we introduce a semi-adaptive stopping rule for KGD based on Proposition 4. Define  $t^* := t_{D,\beta}^* \in [1, T]$  to be the largest integer satisfying

$$\mathcal{W}_{D,t} \leq C'_2 \begin{cases} 2^{r-1/2} t^{-r}, & \text{if } \frac{1}{2} \leq r \leq \frac{3}{2}, \\ t^{-r} + 4\kappa^2 t^{-1/2} |D|^{-1/2}, & \text{if } r > \frac{3}{2}, \end{cases} \quad (34)$$

where  $C'_2 := \max\{\tilde{C}, (2(\beta + 1)\tilde{C})^{-1}C'_1\}$ . It is easy to see that the left side of (34) increases with  $t$  while the right side of (34) decreases with  $t$ . Therefore, the definition of  $t^*$  shows that

$$\mathcal{W}_{D,t} \leq C'_2 \begin{cases} 2^{r-1/2} t^{-r}, & \text{if } \frac{1}{2} \leq r \leq \frac{3}{2}, \\ t^{-r} + 4\kappa^2 t^{-1/2} |D|^{-1/2}, & \text{if } r > \frac{3}{2}, \end{cases} \forall t \leq t^*, \quad (35)$$

and

$$\mathcal{W}_{D,t} \geq C'_2 \begin{cases} 2^{r-1/2} t^{-r}, & \text{if } \frac{1}{2} \leq r \leq \frac{3}{2}, \\ t^{-r} + 4\kappa^2 t^{-1/2} |D|^{-1/2}, & \text{if } r > \frac{3}{2}, \end{cases} \forall t > t^*. \quad (36)$$

The following proposition presents the relation between  $\hat{t}$  and  $t^*$  and provides an upper bound for  $\hat{t}$ .

**Proposition 5** *Let  $0 < \delta < 1$ . For*

$$t_0 = \tilde{c} \log^{a(\sigma)} \frac{16}{\delta} \begin{cases} (|D|/L)^{\frac{1}{2r}}, & \text{if } \sigma_\ell = 0, \ell \geq L + 1, \\ |D|^{\frac{1}{2r+s}}, & \text{if } \sigma_\ell \leq c_0 \ell^{-1/s}, \\ (|D|/\sqrt{\log |D|})^{\frac{1}{2r}}, & \text{if } \sigma_\ell \leq c_1 e^{-c_2 \ell^2}, \end{cases} \quad (37)$$

with some  $\tilde{c}$  depending only on  $\kappa, M, \delta$ , and  $\gamma$  and  $a(\sigma) := -\frac{s}{2r+s}$  when  $\sigma_\ell \leq c_0 \ell^{-1/s}$  and  $a(\sigma) = 0$  otherwise, if Assumptions 1 and 2 hold with  $r \geq 1/2$ , then with confidence  $1 - \delta$ , there holds

$$\max\{\hat{t}, t_0\} \leq t^* \leq T \quad (38)$$

and

$$\begin{aligned} & \max\{\|f_{D,t^*} - f_\rho\|_\rho, \|f_{D,t^*} - f_\rho\|_D, (t^*)^{1/2}\|f_{D,t^*} - f_\rho\|_K\} \\ & \leq \tilde{C}' \log^2 \frac{16}{\delta} \begin{cases} (|D|/L)^{-1/2}, & \text{if } \sigma_\ell = 0, \ell \geq L+1, \\ |D|^{-r/(2r+s)}, & \text{if } \sigma_\ell \leq c_0 \ell^{-1/s}, \\ (|D|/\sqrt{\log |D|})^{-1/2}, & \text{if } \sigma_\ell \leq c_1 e^{-c_2 \ell^2}, \end{cases} \end{aligned} \quad (39)$$

where  $\tilde{C}'$  is a constant independent of  $|D|, t$  or  $\delta$ .

Since  $t_0 \leq t^*$ , we get from (39) that

$$\begin{aligned} & \|f_{D,t^*} - f_\rho\|_K \leq t_0^{-1/2} \tilde{C}' \log^2 \frac{16}{\delta} \begin{cases} (|D|/L)^{-1/2}, & \text{if } \sigma_\ell = 0, \ell \geq L+1, \\ |D|^{-r/(2r+s)}, & \text{if } \sigma_\ell \leq c_0 \ell^{-1/s}, \\ (|D|/\sqrt{\log |D|})^{-1/2}, & \text{if } \sigma_\ell \leq c_1 e^{-c_2 \ell^2} \end{cases} \\ & \leq \tilde{C}'_1 \log^2 \frac{16}{\delta} \begin{cases} (|D|/L)^{-\frac{(1-1/2r)}{2}}, & \text{if } \sigma_\ell = 0, \ell \geq L+1, \\ |D|^{-\frac{r-1/2}{2r+s}}, & \text{if } \sigma_\ell \leq c_0 \ell^{-1/s}, \\ \left(\frac{|D|}{\sqrt{\log |D|}}\right)^{-\frac{(1-1/2r)}{2}}, & \text{if } \sigma_\ell \leq c_1 e^{-c_2 \ell^2}, \end{cases} \end{aligned}$$

which coincides with the bound derived in Corollary 3, where  $\tilde{C}'_1$  is a constant independent of  $\delta, |D|, t$ . Proposition 5 derives optimal generalization error bounds for KGD equipped with the proposed semi-adaptive stopping rule. Furthermore, it presents an upper bound of  $\hat{t}$ , which will play a crucial role in verifying the optimality of the BSP rule in Definition 1.

### 3.3 Optimal generalization error bounds for KGD with HSS

In this subsection, we provide theoretical verifications for the proposed parameter selection strategy. First, we derive the optimal generalization error bounds for KGD with BSP defined by Definition 1.

**Theorem 6** *Let  $0 < \delta < 1$  and  $0 < \beta \leq \kappa^{-1}$ . Under Assumption 1 and Assumption 2 with  $r \geq 1/2$ , if  $\hat{t}$  is defined by Definition 1 with  $\tilde{C} \geq 32\sqrt{2}(1+\beta)(\kappa M + \gamma)$ , then with confidence  $1 - \delta$ , there holds*

$$\max\{\|f_{\hat{t},\beta,D} - f_\rho\|_\rho, \|f_{\hat{t},\beta,D} - f_\rho\|_D\} \leq C \log^4 \frac{16}{\delta} \begin{cases} \frac{\sqrt{L} \log |D|}{\sqrt{|D|}}, & \text{if } \sigma_\ell = 0, \ell \geq L+1, \\ |D|^{-r/(2r+s)}, & \text{if } \sigma_\ell \leq c_0 \ell^{-1/s}, \\ \frac{\log |D|}{\sqrt{|D|}}, & \text{if } \sigma_\ell \leq c_1 e^{-c_2 \ell^2}, \end{cases} \quad (40)$$

and

$$\|f_{\hat{t},\beta,D} - f_\rho\|_K \leq C \log^4 \frac{16}{\delta} \begin{cases} \left(\frac{\sqrt{L} \log |D|}{\sqrt{|D|}}\right)^{1-1/2r}, & \text{if } \sigma_\ell = 0, \ell \geq L+1, \\ |D|^{-\frac{r-1/2}{2r+s}}, & \text{if } \sigma_\ell \leq c_0 \ell^{-1/s}, \\ \left(\frac{\log |D|}{\sqrt{|D|}}\right)^{(1-1/2r)}, & \text{if } \sigma_\ell \leq c_1 e^{-c_2 \ell^2}, \end{cases} \quad (41)$$

where  $C$  is a constant independent of  $|D|$  or  $\delta$ .

Table 1: Comparison of different parameter selection methods

Comparison of parameter selection methods for KGD					
	Methods	generalization error bound	Ada. to kernel	Ada. to function	Ada. to norm $\ \cdot\ _\rho$ and $\ \cdot\ _K$
Information entropy method	<i>AIC</i> (Demjanov et al., 2012)	N/A	✓	×	×
	<i>BIC</i> (Demjanov et al., 2012)	N/A	✓	×	×
Splitting method	<i>HO</i> (Caponnetto and Yao, 2010)	Optimal	✓	✓	×
	<i>CV</i> (Györfi et al., 2002)	Optimal	✓	✓	×
	<i>LOO</i> (Zhang, 2003)	Sub-optimal	✓	✓	×
Bias-variance analysis method	<i>BP</i> (Lu et al., 2020)	Near optimal	✓	✓	×
	<i>LP</i> (Blanchard et al., 2019)	Near-optimal	✓	✓	✓
	<i>ESR</i> (Raskutti et al., 2014)	Optimal	✓	×	×
	<i>DP</i> (Celisse and Wahl, 2021)	Sub-optimal	✓	✓	×
Ours	<i>BSP</i>	Optimal	✓	✓	✓

Note: “Ada.” represents adaptive. “N/A” indicates that no relevant literature related to KGD was found.

Theorem 6 shows that, for polynomial decayed  $L_K$ , KGD with BSP achieves the optimal generalization error bounds of KGD in Corollary 3. Table 1 provides a comparison of different parameter selection strategies for KGD in terms of theoretical performance. We have made the following observations. All methods are adaptive to the kernel, but only HO (Caponnetto and Yao, 2010), CV (Györfi et al., 2002), ESR (Raskutti et al., 2014), and BSP achieve optimal generalization error bounds. Notably, the splitting method does not adapt to the error metric. ESR for KGD does not adapt to the regularity of  $f_\rho$  since it only holds for  $r = 1/2$ . In fact, it behaves similarly to the semi-adaptive stopping rule defined by (34). For BP proposed in (De Vito et al., 2010; Lu et al., 2020) and DP proposed in (Celisse and Wahl, 2021), neither adapts to the error metrics, suggesting that different norms require distinct parameter selection strategies. Only the LP proposed in (Blanchard et al., 2019) and BSP can adapt to the regularity index  $r$ , capacity index  $s$  and also the error metrics. However, LP involves recurrent comparisons on the numerical side and introduces an additional logarithmic term in the generalization error bound, resulting in a gap between Corollary 3 and (Blanchard et al., 2019, Theorem 1). In a recent work (Lin, 2024), a novel Lepskii-type principle was designed for kernel ridge regression (KRR), deriving optimal generalization error bounds. The problem is, however, that due to the saturation phenomenon of KRR (Bauer et al., 2007; Gerfo et al., 2008), the generalization error bounds saturate at  $r \leq 1$ , meaning that larger  $r$  no more implies better generalization error bounds. Our theoretical results in Theorem 6 show that BSP adapts to the regularity index  $r \in [1/2, \infty)$ , capacity index  $s \in (0, 1]$  and different metrics of error. This implies that with a unified parameter selection strategy, optimal generalization error bounds hold for all  $r \in [1/2, \infty)$ ,  $s \in (0, 1]$  under three different norms:  $\|\cdot\|_\rho$ ,  $\|\cdot\|_D$  and  $\|\cdot\|_K$ , simultaneously. This demonstrates the power of BSP, which fully exploits the iterative nature of KGD.

Theorem 6 presents the feasibility and optimality for KGD with BSP. A key point is that the assertions hold for any  $\tilde{C} \geq \tilde{C}_0 := 32\sqrt{2}(1 + \beta)(\kappa M + \gamma)$ . On one hand, it can be found in our proof that the constant  $\tilde{C}_0$  is a little bit pessimistic. We believe that it can be reduced by using a more delicate analysis technique. On the other hand, the best choice of  $\tilde{C}$  is doomed to optimize the parameter selection strategy via minimizing the constant  $C$  in (40) and (41). Recalling that BSP adapts to different metrics of error, HSS then focuses on selecting a good candidate of  $\tilde{C}$  to minimize the error under the  $\|\cdot\|_\rho$  metric (Caponnetto and Yao, 2010). The following corollary that can be derived directly from Theorem 6 presents the theoretical guarantee for KGD with HSS in Algorithm 1.

**Corollary 7** *Let  $0 < \delta < 1$  and  $0 < \beta \leq \kappa^{-1}$ . Under Assumption 1 and Assumption 2 with  $r \geq 1/2$ , if  $t^*$  is given by Algorithm 1 with  $\min_{\hat{C}_j \in C_U} \geq \tilde{C}_0$ , then with confidence  $1 - \delta$ , (40) and (41) hold for  $f_{\hat{t}^*}$ .*

Corollary 7 demonstrates the optimality of the proposed HSS strategy in Algorithm 1. Though an additional assumption  $\min_{\hat{C}_j \in C_U} \geq \tilde{C}_0$  is imposed to the parameter selection strategy that inevitably narrows the range of  $\tilde{C}$  in theory, the estimate of  $\tilde{C}_0$ , as discussed above, is too pessimistic and can be significantly reduced numerically. All the above theoretical results show that without splitting the data, it is possible to design a delicate and fully adaptive parameter selection strategy to equip KGD to achieve its optimal generalization error bounds.

Since our results hold for  $\|\cdot\|_K$  and  $\|\cdot\|_\infty \leq \kappa\|\cdot\|_K$ , we obtain from Theorem 6 the following corollary directly.

**Corollary 8** *Let  $0 < \delta < 1$  and  $0 < \beta \leq \kappa^{-1}$ . Under Assumption 1 and Assumption 2 with  $r \geq 1/2$ , then*

$$\|f_{\hat{t},\beta,D} - f_\rho\|_\infty \leq C\kappa \log^4 \frac{16}{\delta} \begin{cases} \left(\frac{\sqrt{L} \log |D|}{\sqrt{|D|}}\right)^{1-1/2r}, & \text{if } \sigma_\ell = 0, \ell \geq L + 1, \\ |D|^{-\frac{r-1/2}{2r+s}}, & \text{if } \sigma_\ell \leq c_0 \ell^{-1/s}, \\ \left(\frac{\log |D|}{\sqrt{|D|}}\right)^{(1-1/2r)}, & \text{if } \sigma_\ell \leq c_1 e^{-c_2 \ell^2}. \end{cases} \quad (42)$$

Different from describing the generalization error in  $\|\cdot\|_\rho$ , the above corollary derives error bounds in  $\|\cdot\|_\infty$ , which implies the capability of covariate shift problem (Ma et al., 2023), in which the marginal distributions for the test data and training data are different. Actually, for any  $\rho'_X$ , it is easy to derive  $\|\cdot\|_{\rho'} \leq \|\cdot\|_\infty$ . We should highlight that the derived bounds for  $\|\cdot\|_{\rho'}$  is worse than Ma et al. (2023) which involves distribution information in the algorithms. Our results are different from Ma et al. (2023) for tackling the covariant-shift problems. On one hand, our algorithm is distribution-independent and results are independent of the similarity between  $\rho_X$  and  $\rho'_X$ . On the other hand, we introduce a stricter metrics,  $\|\cdot\|_K$  or  $\|\cdot\|_\infty$ , to measure the generalization error which is, at least for  $\|\cdot\|_K$  and polynomial decayed  $L_K$ , optimal in the mini-max sense (Fischer and Steinwart, 2020).

## 4. Numerical analysis

In this section, we perform both toy simulations and two real-world data experiments to demonstrate the numerical properties of KGD with the HSS parameter selection strategy as shown in Algorithm 1, and to verify Theorem 6, Corollary 7, and Corollary 8. Except for the comparison experiments in Simulation 2, all other experiments were executed using Python 3.7 on a PC with an Intel Core i5 2GHz processor. Scripts reproducing these experiments are available at [https://github.com/Ariesoomoon/HSS\\_experiments](https://github.com/Ariesoomoon/HSS_experiments).

### 4.1 Simulation experiments

We conduct three simulations. The first simulation demonstrates the feasibility and power of the proposed adaptive stopping rule BSP. The second simulation illustrates the effectiveness

and superior performance of HSS by comparing it with other parameter selection strategies, including the baseline strategy BS, information entropy methods AIC and BIC, the splitting type strategy HO, and the bias–variance analysis strategies such as BP, LP, ESR, and DP. The third highlights HSS’s capability in overcoming covariate shift. To fully showcase the numerical optimality of HSS, we employ two error metrics:  $L_2$  norm and  $L_\infty$  norm. Each simulation is conducted 10 times for averaging.

We generate  $|D| \in \{200, 400, \dots, 6000\}$  samples for training, where  $|D|$  denotes the cardinality of the dataset  $D = \{(x_i, y_i)\}_{i=1}^{|D|}$ . The inputs  $\{x_i\}_{i=1}^{|D|}$  are independently drawn according to the uniform distribution on the (hyper-)cube  $[0, 1]^d$  with  $d = 1, 3$ . The corresponding outputs are generated from the regression models  $y_i = g_j(x_i) + \varepsilon_i, i = 1, \dots, |D|, j = 1, 2$ , where  $\varepsilon_i$  is the independent Gaussian noise  $\mathcal{N}(0, \sigma^2)$  with  $\sigma = 0.6$ ,

$$g_1(x) := \begin{cases} x, & \text{if } 0 \leq x \leq 0.5, \\ 1 - x, & \text{if } 0.5 < x, \end{cases} \quad (43)$$

and

$$g_2(\|x\|_2) := \begin{cases} (1 - \|x\|_2)^6 (35\|x\|_2^2 + 18\|x\|_2 + 3), & \text{if } 0 \leq \|x\|_2 \leq 1, x \in \mathbb{R}^3, \\ 0, & \text{if } \|x\|_2 > 1. \end{cases} \quad (44)$$

Furthermore, testing samples  $\{(x'_i, y'_i)\}_{i=1}^{|D'|}$  with  $|D'| = 500$  are generated, where  $\{x'_i\}_{i=1}^{|D'|}$  are drawn independently according to the uniform distribution and  $y'_i = g_j(x'_i), j = 1, 2$ . The adopted kernel function is  $K_1(x, x') = 1 + \min(x, x')$  for  $d = 1$  and  $K_2(x, x') = h(\|x - x'\|_2)$  with

$$h(\|x\|_2) := \begin{cases} (1 - \|x\|_2)^4 (4\|x\|_2 + 1), & \text{if } 0 < \|x\|_2 \leq 1, x \in \mathbb{R}^3, \\ 0, & \text{if } \|x\|_2 > 1, \end{cases} \quad (45)$$

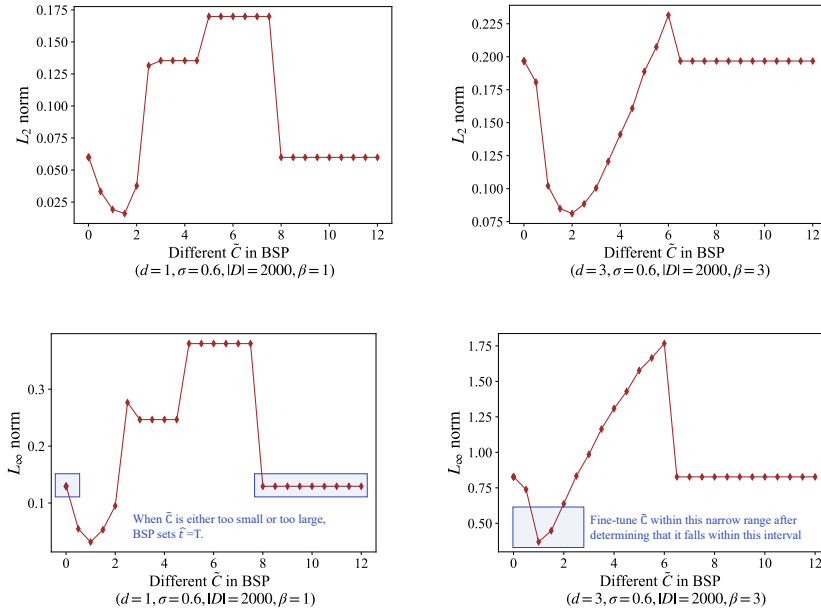
for  $d = 3$ . It can be found in (Wu, 1995; Schaback and Wendland, 2006) that  $g_1 \in W_1^1$  and  $g_2 \in W_3^4$ , where  $W_d^\alpha$  denotes the  $\alpha$ -order Sobolev space on  $[0, 1]^d$ ;  $K_1$  and  $K_2$  are reproducing kernels for  $W_1^1$  and  $W_3^2$ , and  $g_1 \in \mathcal{H}_{K_1}$  and  $g_2 \in \mathcal{H}_{K_2}$ , respectively. Then, the KGD algorithm using the kernels  $K_1$  and  $K_2$  is applied to fit the training samples.

We mention that in all simulations, the ratio of training samples  $D_{tr,L}$  to validation samples  $D_{val,L}$  among the  $L$  selected samples for HSS is fixed at 7:3. The same ratio is applied to other bias–variance analysis methods that require constant parameter selection. For HO, the ratio of training to validation samples is fixed at 1:1. To ensure a fair comparison, the step size  $\beta$  for parameter selection methods in all toy simulations is set to the same value:  $\beta = 1$  for  $d = 1$  and  $\beta = 3$  for  $d = 3$ .

#### 4.1.1 SIMULATION 1: FEASIBILITY AND POWER OF BSP

In this simulation, we conducted two sets of experiments. First, we fixed the total data size  $|D| = 2000$  and observed how two different norms varied with the constant  $\tilde{C}$  of BSP. Second, we examined the range where the optimal  $\tilde{C}$  (denoted as  $\tilde{C}_{j^*}$ ) and the optimal  $t$  (denoted as  $\hat{t}^*$ ) are located across different data scales. There are two main observations from this simulation.

First, in Figure 3, both the  $L_2$  norm and  $L_\infty$  norm exhibit a global minimum with respect to  $\tilde{C}$ , demonstrating the feasibility of using BSP to equip KGD by selecting  $\tilde{C}$ . The similar behavior across different norms highlights the power of BSP. Note that in Figure 3, the two sides of each subplot represent cases where  $\tilde{C}$  is either too large or too small, resulting in  $\hat{t}^*$  being determined as  $T$  by BSP.


 Figure 3: Relation between the  $L_2$  norm/ $L_\infty$  norm and the constant  $\tilde{C}$ .

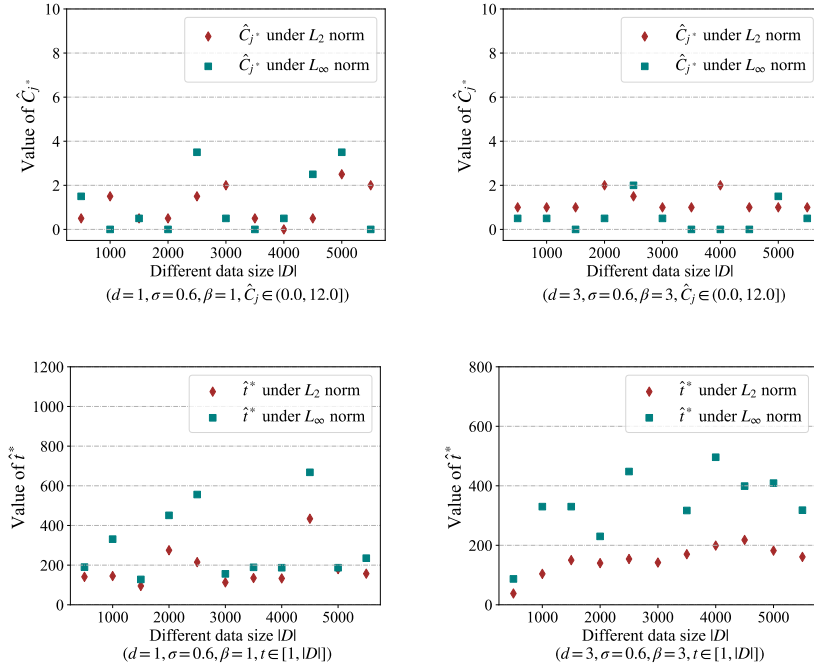
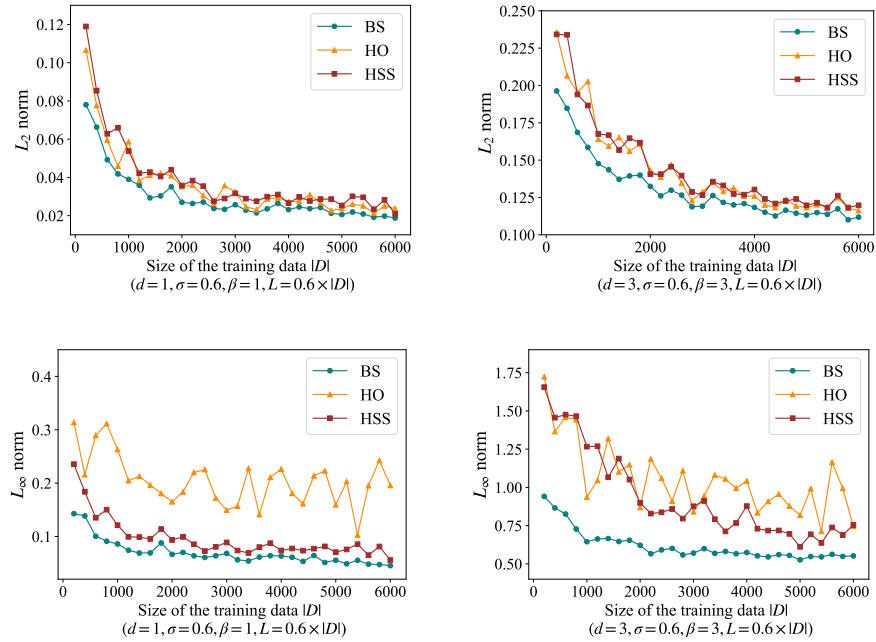
Second, we observe that the optimal  $\tilde{C}$  falls within a relatively narrow range ( $[0, 4]$ ), making it easier to pinpoint. This suggests an efficient parameter selection approach: first, use a logarithmic scale to quickly identify the rough range of  $\tilde{C}$  (i.e., selecting  $\tilde{C} \in \{0, 2^0, 2^1, 2^2, \dots\}$ ), and then refine the selection within that range using a uniform scale (i.e., selecting  $\tilde{C} \in \{0.001, 0.002, \dots\}$ ). This process, referred to as log-uniform parameter selection, was used in our experiments, with the final selection interval for  $\tilde{C}$  set to  $2^{-10}$  (under the uniform scale).

It is important to emphasize that this parameter selection process is not suitable for directly selecting  $\hat{t}^*$ , as we observe that  $\hat{t}^*$  spans a much wider range  $[0, 800]$  compared to  $\hat{C}_j^*$ 's  $[0, 4]$ , as shown in Figure 4, and the generalization error changes gradually with respect to  $t$ , as seen in Figure 1.

#### 4.1.2 SIMULATION 2: EFFECTIVENESS AND SUPERIOR PERFORMANCE OF HSS

In this simulation, we demonstrate the computational efficiency and prediction performance of HSS, thereby validating Theorem 6 and Corollary 7.

Figure 5 compares the prediction performance of BS, HO, and HSS across different data scales, with  $L$  in HSS fixed at  $0.6|D|$ . We observe that under the  $L_2$  norm, the performance of HSS is comparable to HO, both of which are close to BS. However, under the  $L_\infty$  norm, HSS significantly outperforms HO and is closer to the performance of BS. This demonstrates that the adaptive stopping rule BSP can determine a high-quality step  $\hat{t}^*$  based on a well-chosen constant  $\tilde{C}$ , thereby validating our Theorem 6. It highlights the effectiveness and advantages of HSS, particularly its adaptability to different norms, thereby supporting Corollary 7.


 Figure 4: Range of  $\hat{C}_j^*$  under BSP and range of  $\hat{t}^*$  under BS (results from a single experiment).

 Figure 5: Generalization performance of BS, HO, and HSS (where  $L$  in HSS is fixed at  $0.6|D|$ ).

Furthermore, we compared HO, AIC, BIC, HSS and other bias–variance analysis methods in terms of efficiency and accuracy. Results of BP with the constant  $C_{BP}$  from Lu et al. (2020) and ESR with the constant  $C_{ESR}$  from Raskutti et al. (2014) are also presented. Due to the significant memory consumption required for BP and LP, all results in the following were generated using Python 3.7 (Ubuntu 18.04) on a system equipped with an NVIDIA RTX 4090 (24GB) GPU, a 16-core Intel Xeon Platinum 8352V processor (2.10GHz), and 120GB of RAM. The comparison is limited to data scales of 1000 and 1200, with dimensions  $d = 1$  and  $d = 3$ . Each result is conducted 10 times for averaging.

Table 2: Experiment settings for all bias–variance analysis methods in Table 3 and Table 4

Settings	Details	Settings	Details
Number of alternative parameters	24	Step size	$\beta = 1$ for $d = 1$ , $\beta = 3$ for $d = 3$
Parameter selection interval	0.05	Training data size $ D $	1000, 1200
Optimal parameter was selected	Yes	Testing data size $ D' $	500
Number of trials	10	Accuracy metric	$L_2$ norm, $L_\infty$ norm
Maximum number of iterations	$T =  D $	Efficiency metric	Maximum memory usage (MMU), Time (s)

We carefully designed the experiments to ensure a fair comparison, with the specific settings detailed in Table 2. For accuracy, we used the  $L_2$  norm and  $L_\infty$  norm, while for efficiency, we measured the execution time and the maximum memory usage (MMU) and during the execution of each algorithm. Both execution time and MMU were recorded individually.

Table 3: Numerical performance of different parameter selection methods when  $|D| = 1000$ 

Numerical performance of different parameter selection methods								
Methods	$d = 1$				$d = 3$			
	$L_2$ norm	$L_\infty$ norm	Time (s)	MMU (GB)	$L_2$ norm	$L_\infty$ norm	Time (s)	MMU (GB)
HO	0.0587	0.2630	1.03	0.43	0.1641	0.9370	15.98	0.54
AIC	0.0742	0.2407	7.26	0.66	0.1738	1.0100	110.76	0.80
BIC	0.0750	0.2995	8.85	0.65	0.2356	1.0573	109.75	0.81
BP	0.0643	0.1817	924.71	52.40	0.1680	1.0030	1081.37	53.38
<i>Use <math>C_{BP}</math> in (Lu et al., 2020)</i>	<b>0.0528</b>	<b>0.1299</b>	512.08	52.62	0.2095	1.7912	533.16	52.94
LP	0.0658	0.2394	1618.29	76.65	<b>0.1631</b>	0.9624	1543.62	75.79
ESR	0.0598	0.2604	4.88	0.92	0.1632	1.0001	93.09	1.03
<i>Use <math>C_{ESR}</math> in Raskutti et al. (2014)</i>	0.0660	<b>0.1599</b>	4.00	0.47	0.2085	<b>0.7784</b>	24.23	27.48
DP	<b>0.0566</b>	0.2788	4.32	0.49	<b>0.1617</b>	<b>0.9307</b>	87.01	0.62
HSS with $L =  D $	<b>0.0506</b>	<b>0.1216</b>	8.71	0.51	<b>0.1571</b>	<b>0.8633</b>	108.17	0.62

**Note:** The results for each accuracy metric are highlighted in red, blue, and green to denote the best, second-best, and third-best performances, respectively. This also applies to Table 4.

The detailed results are shown in Table 3 and Table 4, where  $L$  in HSS is fixed at  $|D|$ . In terms of accuracy, HSS performs similarly to HO under the  $L_2$  norm but significantly better under the  $L_\infty$  norm, further demonstrating the superior performance of HSS. Regarding efficiency, while HSS is slightly less efficient than HO, its performance remains within an acceptable range. We also observe that the running time of BP is substantially higher than that of HSS, as BP requires item-wise comparisons at each step  $t$  for every constant, whereas HSS only performs two successive iterations. When comparing the results of ESR and BP using the selected constant  $\tilde{C}$  with those using the fixed constants  $C_{ESR}$  and  $C_{BP}$ ,

Table 4: Numerical performance of different parameter selection methods when  $|D| = 1200$ 

Numerical performance of different parameter selection methods								
Methods	$d = 1$				$d = 3$			
	$L_2$ norm	$L_\infty$ norm	Time (s)	MMU (GB)	$L_2$ norm	$L_\infty$ norm	Time (s)	MMU (GB)
HO	<b>0.0384</b>	0.2046	1.52	0.45	0.1594	1.0457	21.77	0.60
AIC	0.0439	0.1548	11.58	0.68	0.1503	1.0330	158.02	0.87
BIC	0.0485	0.2439	12.50	0.68	0.2169	<b>1.0292</b>	163.58	0.92
BP	0.0423	0.1346	1524.22	91.37	0.1513	1.0835	1788.85	91.48
<i>Use <math>C_{BP}</math> in (Lu et al., 2020)</i>	0.0456	<b>0.1164</b>	886.35	90.97	0.2050	1.7753	882.45	90.20
LP	0.0418	<b>0.1249</b>	1604.03*	76.32*	0.1531	1.0692	1750.27*	76.34*
ESR	<b>0.0391</b>	0.1906	7.42	0.95	<b>0.1494</b>	1.0864	133.70	1.06
<i>Use <math>C_{ESR}</math> in Raskutti et al. (2014)</i>	0.0566	0.1398	6.50	0.54	0.2062	<b>0.7983</b>	38.86	0.66
DP	0.0606	0.1635	6.90	0.51	<b>0.1503</b>	1.1473	123.31	0.65
HSS with $L =  D $	<b>0.0393</b>	<b>0.1137</b>	12.26	0.51	<b>0.1492</b>	<b>0.8180</b>	158.00	0.64

**Note:** When the data size is 1200, the LP calculation fails to run due to excessive memory usage (117 GB, which is 97.5% of the system's total 120 GB of memory). We modified the code to release as much memory as possible during execution, allowing it to run normally. Results from this modified code for LP are denoted with \*.

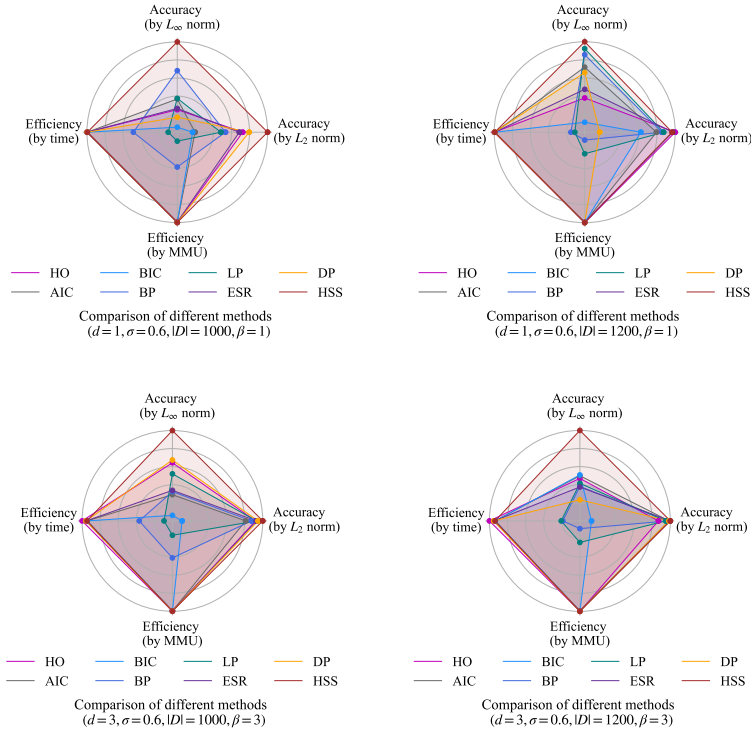


Figure 6: Illustration of the numerical performance of methods presented in Tables 3 and 4.

we found that in most cases, using fixed  $\tilde{C}$  did not yield results as good as those obtained through parameter selection. This indicates that while ESR and BP exhibit good theoretical performance, their numerical effectiveness depends heavily on the quality of  $\tilde{C}$ .

To provide a clear overview of the comparative results for all methods presented in the above two tables, we created a radar chart, as shown in Figure 6. We modified the indicators MMU and Time to be expressed similarly to accuracy; in this chart, values closer to the

edge (or larger areas) represent better performance. From Figure 6, we make the following observations: (1) HSS demonstrates the best overall performance across all four indicators of accuracy and efficiency. Its advantage over other algorithms is particularly evident in  $L_\infty$  norm. (2) While HO, AIC, BIC, ESR and DP perform well in terms of efficiency, their accuracy is generally inferior to HSS. (3) BP and LP perform significantly worse in terms of both running time and MMU, primarily due to their reliance on item-wise comparisons for each given constant (see (16) and (17)).

The results of the radar chart demonstrate that among information entropy methods, splitting methods and bias-variance analysis methods, HSS exhibits superior performance in both efficiency and accuracy.

#### 4.1.3 SIMULATION 3: HSS OVERCOMING COVARIATE SHIFT

This simulation demonstrates that HSS effectively addresses the covariate shift problem and thus validates Corollary 8, thereby contributing to the existing literature on covariate shift in RKHS-based nonparametric regression (Ma et al., 2023). Specifically, Ma et al. (2023) focuses on kernel ridge regression (KRR) and proposes a variant known as the truncated-reweighted KRR estimator, which achieves minimax rate-optimality (Ma et al., 2023, Theorem 4). In contrast, we focus on KGD.

For simplicity, we set  $d = 1$  and assume  $\{x'_i\}_{i=1}^{|D'|}$  are independently drawn according to the uniform distribution on the (hyper-)cube  $[0, b]$  with  $b \in \{1.1, 1.2, \dots, 1.5\}$ . We use Kullback-Leibler (KL) divergence to quantify the distributional difference. For continuous probability distributions  $P$  and  $Q$ , the KL divergence from  $Q$  to  $P$ , denoted as  $\mathbb{D}_{\text{KL}}(P\|Q)$ , is defined as  $\mathbb{D}_{\text{KL}}(P\|Q) = \int_{-\infty}^{\infty} p(\mathbf{x}) \ln \left( \frac{p(\mathbf{x})}{q(\mathbf{x})} \right) d\mathbf{x}$ , where  $p(\mathbf{x})$  and  $q(\mathbf{x})$  are the probability density functions of  $P$  and  $Q$ , respectively. To calculate KL divergence (hereafter denoted as  $\mathbb{D}_{\text{KL}}$ ), we use kernel density estimation (with a bandwidth of 0.05) to obtain the probability density functions and Gauss-Legendre quadrature for integration.

Figure 7 presents the results under covariate shift. Figures 7(a) and 7(b) show that HSS consistently outperforms HO, where “ $\Delta L_2$  norm (%)” represents the change in the  $L_2$  norm under covariate shift relative to the  $L_2$  norm without shift, and “ $\Delta L_\infty$  norm (%)” carries a similar meaning. Figures 7(c) and 7(d) provide detailed results for both HSS and HO across 10 trials using boxplots, revealing that HSS exhibits smaller fluctuations as  $\mathbb{D}_{\text{KL}}$  varies. These results confirm HSS’s robustness in handling covariate shift, thereby supporting the theoretical optimal generalization error bound guarantee under the  $\|\cdot\|_\infty$  metric as stated in Corollary 8.

We further explored HSS’s performance with different  $L$  under covariate shift, as shown in Figure 8. The dashed line represents HSS’s performance when  $L = 0.5|D|$ . We found that using a smaller  $L$  often provides a slight advantage in prediction performance compared to a larger  $L$  under covariate shift, especially in the  $L_\infty$  norm. This may be because using less training data to select  $L$  may help avoid overfitting, thus improving performance under covariate shift.

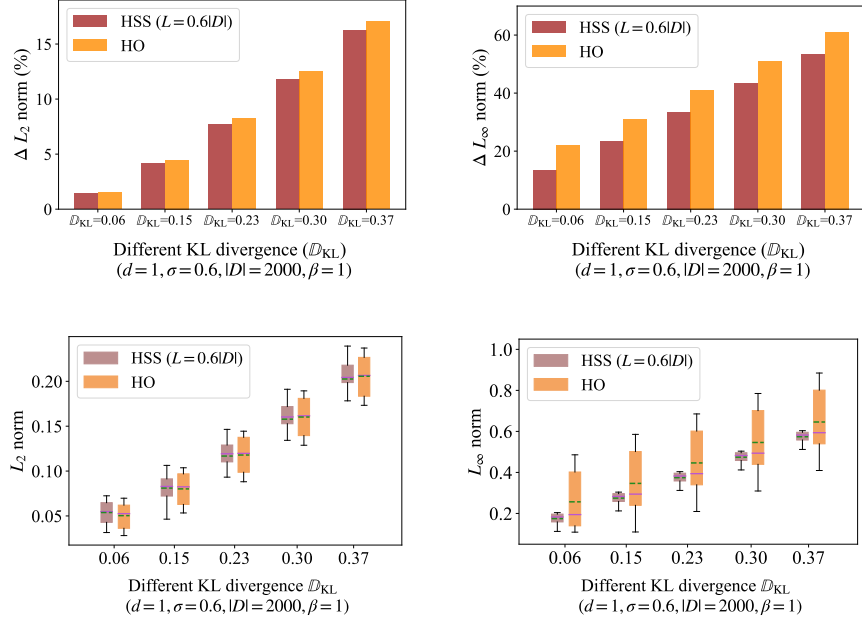


Figure 7: Results under covariate shift.

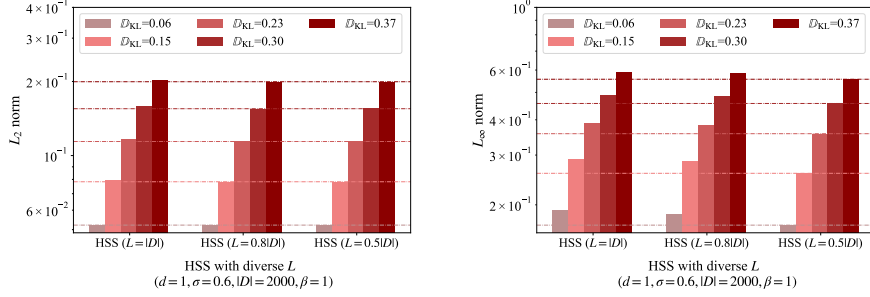


Figure 8: Results under covariate shift.

## 4.2 Real data examples

Lastly, we evaluate the proposed HSS on two real-world datasets under the  $L_2$  norm. These datasets pertain to the magnetic field information on the Earth’s surface at varying latitudes, longitudes, and altitudes, specifically the magnetic total intensity dataset and the magnetic declination dataset. They are crucial for various applications, including navigation, positioning, geological exploration, and more. These two datasets are collected from the website [https://geomag.bgs.ac.uk/data\\_service/models\\_compass/igrf\\_calc.html](https://geomag.bgs.ac.uk/data_service/models_compass/igrf_calc.html), whose geomagnetic field information is provided by the 13th generation of IGRF (IGRF-13) (Alken et al., 2021) based on observations recorded by satellites and ground observatories. We only use the latitude  $\phi$ , longitude  $\theta$ , altitude  $h$ , corresponding total intensity (nT) and declination (degree) attributes on August 15th, 2024 in experiment.

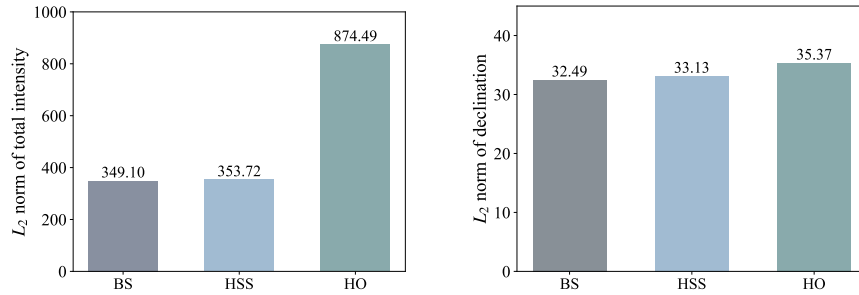


Figure 9: Generalization performance of BS, HO, and HSS for the total intensity data and declination data of magnetic field. In HSS,  $L$  is set to  $0.8|D|$  for the total intensity data and  $0.9|D|$  for the declination data.

For generating training samples, we first draw 2000 samples according to the uniform distribution on the (hyper-)cube  $[-1, 1]^d$  with  $d = 3$ , and then use the same data processing and collection strategy as in (Liu et al., 2024) to collect total intensity and declination data from the above website. We collect 2664 samples as testing samples from locations where  $\phi$  and  $\theta$  are sampled every five degrees and  $h$  is fixed at 0km for visualizing them in Miller cylindrical projection. Similar to Liu et al. (2024), we introduce truncated Gaussian noise with a standard deviation  $\sigma = 500$  to the training samples of total intensity data and  $\sigma = 20$  to the training samples of declination data, resulting in noisy data. We apply the same parameter selection for the constant  $\tilde{C}$  in HSS as used in the toy simulations. For a fair comparison among HSS, BS, and HO, their step size  $\beta$  is set to 45 for total intensity data and set to 20 for declination data. Each experiment is conducted five times for averaging.

We set  $L = 0.8 \times 2000$  for the magnetic total intensity data and  $L = 0.9 \times 2000$  for the magnetic declination data in HSS. Figure 9 shows that HSS performs nearly the same as BS and better than HO (especially on the total intensity data), which demonstrates the advantage of HSS. Figure 10 presents a visualization of global maps related to total intensity, including the total intensity data given by IGRF-13 (Alken et al., 2021), total intensity fitted data by HO and HSS. We have highlighted two areas with light white rectangles in each map to highlight their difference. Compared with the ground truth, HSS provides predictions closer to those given by IGRF-13.

## 5. Further discussion

The semi-adaptive nature of bias–variance analysis methods and the sub-optimality of information entropy methods limit their effectiveness in parameter selection. In this context, splitting methods—particularly cross-validation and hold-out—remain dominant in practice. However, splitting methods often perform poorly in practice due to wasting a portion of samples to create the validation set. Without discarding any samples, we propose the HSS method that combines the advantages of both bias–variance analysis and splitting methods, achieving optimal generalization error bounds for all the regularity index  $r \in [1/2, \infty)$ , capacity index  $s \in (0, 1]$ , and different metrics of error ( $\|\cdot\|_\rho$ ,  $\|\cdot\|_D$  and  $\|\cdot\|_K$ ).

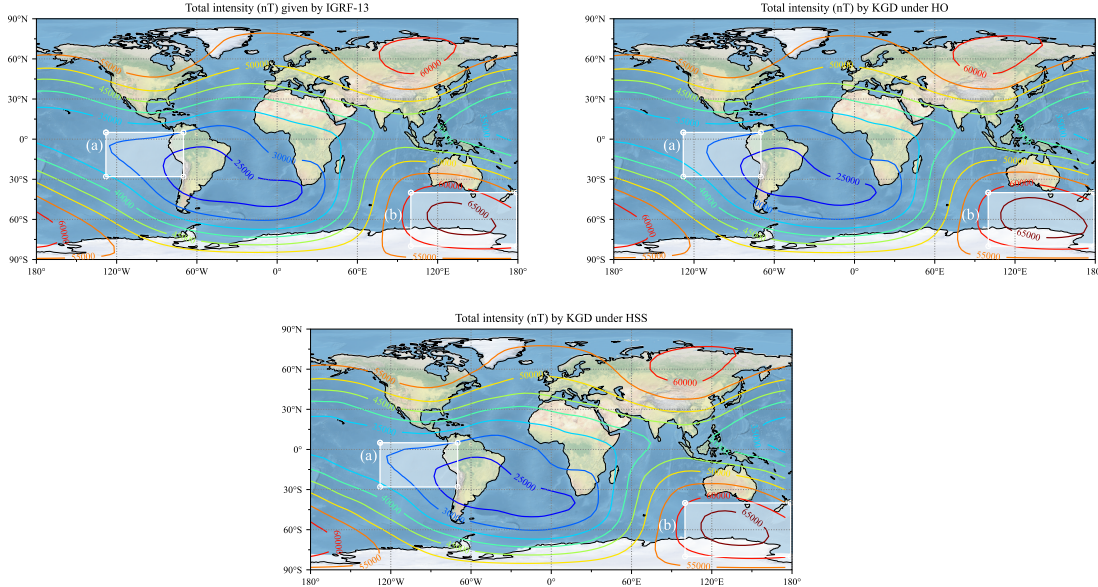


Figure 10: Maps of magnetic total intensity given by IGRF-13 (top panel) and predicted by KGD under HO (middle panel) and KGD under HSS (bottom panel) at the WGS84 ellipsoid surface on August 15th, 2024. The projection used is the Miller cylindrical projection.

Notably, as HSS does not rely on the entire dataset for constant selection, future research could explore its application in distributed learning systems, where each local agent selects constants based on its own local data. Building on the theoretical results in this paper, combining HSS with distributed learning has the potential to contribute to the development of privacy-preserving distributed kernel-based gradient descent algorithms, while maintaining high prediction accuracy.

Furthermore, given the substantial body of research on kernel methods for spherical data (such as the magnetic total intensity data used in our real-data experiments) and the fact that many real-world spherical datasets are acquired through deterministic sampling (e.g., satellite deterministic sampling), investigating a fully adaptive parameter selection strategy for KGD specifically designed for such spherical data would be an interesting direction for future research.

## Acknowledgment

The work is supported partially by the National Natural Science Foundation of China (Grant Numbers 62276209).

## References

Hirotsugu Akaike. A new look at the statistical model identification. *IEEE Trans. Automat. Contr.*, 19(6):716–723, 1974.

- Patrick Alken, Erwan Thébault, Ciarán D Beggan, Hagay Amit, J Aubert, J Baerenzung, TN Bondar, WJ Brown, S Califf, A Chambodut, et al. International geomagnetic reference field: The thirteenth generation. *Earth, Planets and Space*, 73:1–25, 2021.
- Frank Bauer, Sergei Pereverzev, and Lorenzo Rosasco. On regularization algorithms in learning theory. *J. Complex.*, 23(1):52–72, 2007.
- Yoshua Bengio, Ian Goodfellow, and Aaron Courville. *Deep Learning*, volume 1. MIT Press, 2017.
- Gilles Blanchard and Nicole Krämer. Convergence rates of kernel conjugate gradient for random design regression. *Anal. Appl.*, 14(06):763–794, 2016.
- Gilles Blanchard, Peter Mathé, and Nicole Mücke. Lepskii principle in supervised learning. *arXiv preprint arXiv:1905.10764*, 2019.
- Andrea Caponnetto and Ernesto De Vito. Optimal rates for the regularized least-squares algorithm. *Found. Comput. Math.*, 7(3):331–368, 2007.
- Andrea Caponnetto and Yuan Yao. Cross-validation based adaptation for regularization operators in learning theory. *Anal. Appl.*, 8(02):161–183, 2010.
- Alain Celisse and Martin Wahl. Analyzing the discrepancy principle for kernelized spectral filter learning algorithms. *J. Mach. Learn. Res.*, 22:1–76, 2021.
- Olivier Chapelle, Vladimir Vapnik, Olivier Bousquet, and Sayan Mukherjee. Choosing multiple parameters for support vector machines. *Mach. Learn.*, 46:131–159, 2002.
- Gerda Claeskens, Christophe Croux, and Johan Van Kerckhoven. An information criterion for variable selection in support vector machines. *J. Mach. Learn. Res.*, 9:541–558, 2008.
- Ernesto De Vito, Sergei Pereverzyev, and Lorenzo Rosasco. Adaptive kernel methods using the balancing principle. *Found. Comput. Math.*, 10(4):455–479, 2010.
- Sergey Demyanov, James Bailey, Kotagiri Ramamohanarao, and Christopher Leckie. Aic and bic based approaches for svm parameter value estimation with rbf kernels. In *Asian Conference on Machine Learning*, pages 97–112, 2012.
- Marius-Constantin Dinu, Markus Holzleitner, Maximilian Beck, Hoan Duc Nguyen, Andrea Huber, Hamid Eghbal-zadeh, Bernhard A. Moser, Sergei Pereverzyev, Sepp Hochreiter, and Werner Zellinger. Addressing parameter choice issues in unsupervised domain adaptation by aggregation. In *The Eleventh International Conference on Learning Representations*, 2023.
- Heinz Werner Engl, Martin Hanke, and Andreas Neubauer. *Regularization of Inverse Problems*, volume 375. Springer Science & Business Media, 1996.
- Simon Fischer and Ingo Steinwart. Sobolev norm learning rates for regularized least-squares algorithms. *J. Mach. Learn. Res.*, 21(205):1–38, 2020.

- Junichi Fujii, Masatoshi Fujii, Takayuki Furuta, and Ritsuo Nakamoto. Norm inequalities equivalent to heinz inequality. *Proc. Am. Math. Soc.*, 118(3):827–830, 1993.
- L Lo Gerfo, Lorenzo Rosasco, Francesca Odone, E De Vito, and Alessandro Verri. Spectral algorithms for supervised learning. *Neural Comput.*, 20(7):1873–1897, 2008.
- Elke R Gizewski, Lukas Mayer, Bernhard A Moser, Duc Hoan Nguyen, Sergiy Pereverzyev Jr, Sergei V Pereverzyev, Natalia Shepeleva, and Werner Zellinger. On a regularization of unsupervised domain adaptation in rkhs. *Appl. Comput. Harmon. Anal.*, 57:201–227, 2022.
- Zheng-Chu Guo, Shao-Bo Lin, and Ding-Xuan Zhou. Learning theory of distributed spectral algorithms. *Inverse Probl.*, 33(7):074009, 2017.
- László Györfi, Michael Kohler, Adam Krzyżak, and Harro Walk. *A Distribution-free Theory of Nonparametric Regression*, volume 1. Springer, 2002.
- Omar Hagrass, Bharath Sriperumbudur, and Bing Li. Spectral regularized kernel two-sample tests. *Ann. Statist.*, 52(3):1076–1101, 2024.
- Peter Hall and JS Marron. On variance estimation in nonparametric regression. *Biometrika.*, 77(2):415–419, 1990.
- Ting Hu, Qiang Wu, and Ding-Xuan Zhou. Distributed kernel gradient descent algorithm for minimum error entropy principle. *Appl. Comput. Harmon. Anal.*, 49(1):229–256, 2020.
- Clifford M. Hurvich, Jeffrey S. Simonoff, and Chih-Ling Tsai. Smoothing parameter selection in nonparametric regression using an improved akaike information criterion. *J. R. Stat. Soc. Ser. B Stat. Methodol.*, 60(2):271–293, 1998.
- Raytcho D Lazarov, Shuai Lu, and Sergei V Pereverzev. On the balancing principle for some problems of numerical analysis. *Numer. Math.*, 106:659–689, 2007.
- Shao-Bo Lin. Adaptive parameter selection for kernel ridge regression. *Appl. Comput. Harmon. Anal.*, page 101671, 2024.
- Shao-Bo Lin and Ding-Xuan Zhou. Distributed kernel-based gradient descent algorithms. *Constr. Approx.*, 47(2):249–276, 2018a.
- Shao-Bo Lin and Ding-Xuan Zhou. Optimal learning rates for kernel partial least squares. *J. Fourier. Anal. Appl.*, 24:908–933, 2018b.
- Shao-Bo Lin, Xin Guo, and Ding-Xuan Zhou. Distributed learning with regularized least squares. *J. Mach. Learn. Res.*, 18(1):3202–3232, 2017.
- Shao-Bo Lin, Yunwen Lei, and Ding-Xuan Zhou. Boosted kernel ridge regression: Optimal learning rates and early stopping. *J. Mach. Learn. Res.*, 20(1):1738–1773, 2019.
- Xiaotong Liu, Jinxin Wang, Di Wang, and Shao-Bo Lin. Weighted spectral filters for kernel interpolation on spheres: Estimates of prediction accuracy for noisy data. *SIAM J. Imaging. Sci.*, 17(2):951–983, 2024.

- Shuai Lu, Peter Mathé, and Sergei V Pereverzev. Balancing principle in supervised learning for a general regularization scheme. *Appl. Comput. Harmon. Anal.*, 48(1):123–148, 2020.
- Cong Ma, Reese Pathak, and Martin J Wainwright. Optimally tackling covariate shift in rkhs-based nonparametric regression. *Ann. Statist.*, 51(2):738–761, 2023.
- Drton Mathias and Plummer Martyn. A bayesian information criterion for singular models. *J. R. Stat. Soc. Ser. B Stat. Methodol.*, 79(2):323–380, 2017.
- Ryuei Nishii. Asymptotic properties of criteria for selection of variables in multiple regression. *Ann. Statist.*, pages 758–765, 1984.
- Garvesh Raskutti, Martin J Wainwright, and Bin Yu. Minimax-optimal rates for sparse additive models over kernel classes via convex programming. *The Journal of Machine Learning Research*, 13(1):389–427, 2012.
- Garvesh Raskutti, Martin J Wainwright, and Bin Yu. Early stopping and non-parametric regression: An optimal data-dependent stopping rule. *J. Mach. Learn. Res.*, 15(1):335–366, 2014.
- Philip T Reiss and R Todd Ogden. Smoothing parameter selection for a class of semiparametric linear models. *J. R. Stat. Soc. Ser. B Stat. Methodol.*, 71(2):505–523, 2009.
- Robert Schaback and Holger Wendland. Kernel techniques: From machine learning to meshless methods. *Acta Numer.*, 15:543–639, 2006.
- Gideon Schwarz. Estimating the dimension of a model. *Ann. Statist.*, pages 461–464, 1978.
- Steve Smale and Ding-Xuan Zhou. Learning theory estimates via integral operators and their approximations. *Constr. Approx.*, 26(2):153–172, 2007.
- Ingo Steinwart and Andreas Christmann. *Support Vector Machines*. Springer Science & Business Media, 2008.
- Yuting Wei, Fanny Yang, and Martin J Wainwright. Early stopping for kernel boosting algorithms: A general analysis with localized complexities. *IEEE Trans. Inf. Theory.*, 65(10):6685–6703, 2019.
- Zongmin Wu. Compactly supported positive definite radial functions. *Adv. Comput. Math.*, 4:283–292, 1995.
- Ganggang Xu, Zuofeng Shang, and Guang Cheng. Distributed generalized cross-validation for divide-and-conquer kernel ridge regression and its asymptotic optimality. *J. Comput. Graph. Stat.*, 28(4):891–908, 2019.
- Yuan Yao, Lorenzo Rosasco, and Andrea Caponnetto. On early stopping in gradient descent learning. *Constr. Approx.*, 26(2):289–315, 2007.
- Tong Zhang. Effective dimension and generalization of kernel learning. *Adv. Neural Inf. Process. Syst.*, 15, 2002.

Tong Zhang. Leave-one-out bounds for kernel methods. *Neural Comput.*, 15(6):1397–1437, 2003.

Yuchen Zhang, John Duchi, and Martin Wainwright. Divide and conquer kernel ridge regression: A distributed algorithm with minimax optimal rates. *J. Mach. Learn. Res.*, 16(1):3299–3340, 2015.

## Appendix A: Operator representations and operator concentrations

The main tool in our analysis is the integral operator approach developed in (Smale and Zhou, 2007; Lin et al., 2017; Guo et al., 2017). Let  $S_D : \mathcal{H}_K \rightarrow \mathbb{R}^{|D|}$  be the sampling operator (Smale and Zhou, 2007) defined by

$$S_D f := (f(x))_{(x,y) \in D}.$$

Its scaled adjoint  $S_D^\top : \mathbb{R}^{|D|} \rightarrow \mathcal{H}_K$  is given by

$$S_D^\top \mathbf{c} := \frac{1}{|D|} \sum_{i=1}^{|D|} c_i K_{x_i}, \quad \mathbf{c} := (c_1, c_2, \dots, c_{|D|})^\top \in \mathbb{R}^{|D|}.$$

Define  $L_{K,D} : \mathcal{H}_K \rightarrow \mathcal{H}_K$  the empirical version of the integral operator  $L_K$  by

$$L_{K,D} f := \frac{1}{|D|} \sum_{(x,y) \in D} f(x) K_x.$$

For an arbitrary  $f \in \mathcal{H}_K$ , it is easy to check

$$\|f\|_D = \|L_{K,D}^{1/2} f\|_K, \quad \text{and} \quad \|f\|_\rho = \|L_K^{1/2} f\|_K. \quad (\text{A1})$$

The gradient descent algorithm (3) can be rewritten as

$$f_{t+1,\beta,D} = f_{t,\beta,D} - \beta \left( L_{K,D} f_{t,\beta,D} - S_D^\top y_D \right) = (I - \beta L_{K,D}) f_{t,\beta,D} + \beta S_D^\top y_D. \quad (\text{A2})$$

Direct computation (Yao et al., 2007; Lin and Zhou, 2018a) yields

$$f_{t,\beta,D} = \sum_{k=0}^{t-1} \beta \pi'_{k+1,\beta}(L_{K,D}) S_D^\top y_D = g_{t,\beta}(L_{K,D}) S_D^\top y_D, \quad (\text{A3})$$

where  $\pi'_{k+1,\beta}(u) := \prod_{\ell=k+1}^{t-1} (1 - \beta u) = (1 - \beta u)^{t-k-1}$ ,  $\pi'_{t,\beta} := 1$  and

$$g_{t,\beta}(u) = \sum_{k=0}^{t-1} \beta \pi'_{k+1,\beta}(u) = \frac{1 - (1 - \beta u)^t}{u}, \quad \forall u > 0. \quad (\text{A4})$$

The operator representation of KGD by (A3) is significant, which will be used throughout the analysis of KGD. The following lemma that is well known in inverse problems (Engl et al., 1996, Chap.6) and nonparametric regression (Bauer et al., 2007; Yao et al., 2007; Lin and Zhou, 2018a) shows some important properties for this representation.

**Lemma A.1** *Let  $g_{t,\beta}$  be defined by (A4). We have*

$$\|L_{K,D} g_{t,\beta}(L_{K,D})\| \leq 1, \quad \frac{1}{t} \|g_{t,\beta}(L_{K,D})\| \leq \beta, \quad (\text{A5})$$

and

$$\|L_{K,D}^v (I - L_{K,D} g_{t,\beta}(L_{K,D}))\| \leq \left( \frac{v}{t\beta} \right)^v, \quad v \geq 0. \quad (\text{A6})$$

Based on the operator representation, we use the operator difference to describe the bias, variance and generalization. The following lemma combines several standard concentration inequalities in (Caponnetto and De Vito, 2007; Blanchard and Krämer, 2016; Guo et al., 2017; Blanchard et al., 2019) (see also (Lin et al., 2019, Lemma 22)).

**Lemma A.2** *Let  $\delta \in (0, 1)$  and  $D$  be a dataset with samples drawn independently according to  $\rho$ . Under (15), with confidence at least  $1 - \delta$ ,*

$$\begin{aligned}\mathcal{S}_{D,t} &\leq C_1^* \left( \frac{\log \max\{1, \mathcal{N}(t^{-1})\}}{t^{-1}|D|} + \sqrt{\frac{\log \max\{1, \mathcal{N}(t^{-1})\}}{t^{-1}|D|}} \right), \\ \mathcal{R}_D &\leq \frac{4\kappa^2}{\sqrt{|D|}} \log \frac{8}{\delta}, \\ \mathcal{P}_{D,t} &\leq 2(\kappa M + \gamma) \mathcal{A}_{D,\lambda} \log(8/\delta),\end{aligned}$$

and

$$\begin{aligned}(1 + 4\eta_{\delta/4})^{-1} \sqrt{\max\{\mathcal{N}(t^{-1}), 1\}} &\leq \sqrt{\max\{\mathcal{N}_D(t^{-1}), 1\}} \\ &\leq (1 + 4\sqrt{\eta_{\delta/4}} \vee \eta_{\delta/4}^2) \sqrt{\max\{\mathcal{N}(t^{-1}), 1\}}\end{aligned}$$

hold simultaneously, where  $C_1^* := \max\{(\kappa^2 + 1)/3, 2\sqrt{\kappa^2 + 1}\}$ ,

$$\mathcal{S}_{D,t} := \|(L_K + t^{-1}I)^{-1/2}(L_K - L_{K,D})(L_K + t^{-1}I)^{-1/2}\|, \quad (\text{A7})$$

$$\mathcal{R}_D := \|L_K - L_{K,D}\|_{HS}, \quad (\text{A8})$$

$$\mathcal{P}_{D,t} := \left\| (L_K + t^{-1}I)^{-1/2}(L_K f_\rho - S_{D^\top}^\top y_D) \right\|_K, \quad (\text{A9})$$

$\eta_\delta := 2 \log(16/\delta) \sqrt{t}/\sqrt{|D|}$  and  $\|A\|_{HS}$  is the Hilbert-Schmidt norm of the Hilbert-Schmidt operator  $A$ .

From the above lemma, we can derive an upper bound of  $\mathcal{Q}_{D,t}$ .

**Lemma A.3** *For any  $\delta \in (0, 1)$ , if  $C_1^* \mathcal{U}_{D,t,\delta} \leq 1/2$ , then with confidence  $1 - \delta$ , there holds*

$$\mathcal{Q}_{D,t} \leq \sqrt{2}.$$

**Proof** Direct computation yields

$$\begin{aligned}&(L_K + \lambda I)^{1/2}(L_{K,D} + \lambda I)^{-1}(L_K + \lambda I)^{1/2} \\ &= (L_K + \lambda I)^{1/2}[(L_{K,D} + \lambda I)^{-1} - (L_K + \lambda I)^{-1}](L_K + \lambda I)^{1/2} + I \\ &= I + (L_K + \lambda I)^{-1/2}(L_K - L_{K,D})(L_K + \lambda I)^{-1/2}(L_K + \lambda I)^{1/2}(L_{K,D} + \lambda I)^{-1}(L_K + \lambda I)^{1/2}.\end{aligned}$$

We then have from (A7) that

$$\begin{aligned}&\|(L_K + \lambda I)^{1/2}(L_{K,D} + \lambda I)^{-1}(L_K + \lambda I)^{1/2}\| \\ &\leq 1 + \mathcal{S}_{D,t} \|(L_K + \lambda I)^{1/2}(L_{K,D} + \lambda I)^{-1}(L_K + \lambda I)^{1/2}\|.\end{aligned}$$

The only thing remaining is to present a restriction on  $t$  so that  $\mathcal{S}_{D,t} < 1$ . For this purpose, recall Lemma A.2 and get that with confidence  $1 - \delta$ , there holds

$$\mathcal{S}_{D,t} \leq C_1^* \left( \frac{\log \max\{1, \mathcal{N}(t^{-1})\}}{t^{-1}|D|} + \sqrt{\frac{\log \max\{1, \mathcal{N}(t^{-1})\}}{t^{-1}|D|}} \right) \leq C_1^* \mathcal{U}_{D,t,\delta}.$$

Therefore, for any  $t$  satisfying

$$C_1 * \mathcal{U}_{D,t,\delta} \leq 1/2,$$

we have  $\mathcal{Q}_{D,t} \leq \sqrt{2}$ . This completes the proof of Lemma A.3.  $\blacksquare$

From Lemma A.2 and Lemma A.3, we can establish a relation between operator differences and  $\mathcal{W}_{D,t}$ , which is similar as that in (Lin et al., 2019, Lemma 23)

**Lemma A.4** *For any  $0 < \delta < 1$  and  $1 \leq t \leq T$ , under (15), with confidence  $1 - \delta$ , there holds*

$$\mathcal{P}_{D,t} \mathcal{Q}_{D,t} \leq 2\sqrt{2}(\kappa M + \gamma) \mathcal{A}_{D,\lambda} \log \frac{8}{\delta} \leq \sqrt{2} \mathcal{W}_{D,t} \log^2 \frac{16}{\delta}. \quad (\text{A10})$$

**Proof** The first inequality follows from Lemma A.2 and Lemma A.3 directly. We then turn to proving the second inequality in (A10). It follows from Lemma A.2 and (30) that with confidence  $1 - \delta$ ,

$$\mathcal{A}_{D,t} \leq \frac{\sqrt{t}}{|D|} + \frac{\sqrt{\max\{\mathcal{N}_D(t^{-1}), 1\}}(1 + 8\sqrt{t/|D|})}{\sqrt{|D|}} \log \frac{16}{\delta}.$$

Then, we obtain from Lemma A.2 that with confidence  $1 - \delta$ ,

$$\mathcal{P}_{D,t} \leq 2(\kappa M + \gamma) \left( \frac{\sqrt{t}}{|D|} + \frac{\sqrt{\max\{\mathcal{N}_D(t^{-1}), 1\}}(1 + 8\sqrt{t/|D|})}{\sqrt{|D|}} \right) \log^2 \frac{16}{\delta}.$$

Thus, for any  $1 \leq t \leq T$ , we have from Lemma A.3 that with confidence  $1 - \delta$ , there holds

$$\mathcal{P}_{D,t} \mathcal{Q}_{D,t} \leq 2\sqrt{2}(\kappa M + \gamma) \log^2 \frac{16}{\delta} \left( \frac{\sqrt{t}}{|D|} + \frac{\sqrt{\max\{\mathcal{N}_D(t^{-1}), 1\}}(1 + 8\sqrt{t/|D|})}{\sqrt{|D|}} \right).$$

This together with (6) completes the proof of Lemma A.4.  $\blacksquare$

## Appendix B: Proof of propositions and corollaries

In this section, we focus on proving propositions.

**Proof** [Proof of Proposition 2] Due to (22) and (A3), we have

$$f_{t,\beta,D}^\circ = g_{t,\beta}(L_{K,D}) L_{K,D} f_\rho. \quad (\text{B11})$$

Then (26), (16) with  $r \geq 1/2$  and (A1) yield

$$\begin{aligned} \mathcal{B}_{t,\beta,D} &\leq 2\|(L_{K,D} + t^{-1}I)^{1/2}(g_{t,\beta}(L_{K,D})L_{K,D} - I)f_\rho\|_K \\ &\leq 2\|(L_{K,D} + t^{-1}I)^{1/2}(g_{t,\beta}(L_{K,D})L_{K,D} - I)L_K^{r-1/2}\| \|h_\rho\|_\rho. \end{aligned}$$

If  $\frac{1}{2} \leq r \leq 1$ , we then have from Lemma A.1 and the Cordes inequality (Fujii et al., 1993)

$$\|A^\alpha B^\alpha\| \leq \|AB\|^\alpha, \quad 0 \leq \alpha \leq 1 \quad (\text{B12})$$

for all symmetric and positive-definite positive operators  $A$  and  $B$  that

$$\begin{aligned} & \| (L_{K,D} + t^{-1})^{1/2} (g_{t,\beta}(L_{K,D})L_{K,D} - I) L_K^{r-1/2} \| \\ & \leq \| (L_{K,D} + t^{-1})^{1/2} (g_{t,\beta}(L_{K,D})L_{K,D} - I) (L_{K,D} + t^{-1}I)^{r-1/2} \| \mathcal{Q}_{D,t}^{2r-1} \\ & \leq 2^r \mathcal{Q}_{D,t}^{2r-1} (\|L_{K,D}^r (g_{t,\beta}(L_{K,D})L_{K,D} - I)\| + t^{-r} \|g_{t,\beta}(L_{K,D})L_{K,D} - I\|) \\ & \leq 2^r \mathcal{Q}_{D,t}^{2r-1} ((r/\beta)^r + 1) t^{-r}. \end{aligned}$$

If  $r > 1$ , we obtain from Lemma A.1 again, the bounds  $\|L_{K,D}\| \leq \kappa^2$ ,  $\|L_K\| \leq \kappa^2$ , and the following Lipschitz inequality (Blanchard and Krämer, 2016)

$$\begin{aligned} & \|L_{K,D}^{r-1/2} - L_K^{r-1/2}\| \leq \|L_{K,D}^{r-1/2} - L_K^{r-1/2}\|_{HS} \\ & \leq \max\{1, (r-1/2)\kappa^{2r-3}\} \|L_{K,D} - L_K\|_{HS}^{\min\{1, r-1/2\}} \end{aligned} \quad (\text{B13})$$

that

$$\begin{aligned} & \| (L_{K,D} + t^{-1})^{1/2} (g_{t,\beta}(L_{K,D})L_{K,D} - I) L_K^{r-1/2} \| \\ & \leq \| (L_{K,D} + t^{-1})^{1/2} L_{K,D}^{r-1/2} (g_{t,\beta}(L_{K,D})L_{K,D} - I) \| \\ & \quad + \| (L_{K,D} + t^{-1})^{1/2} (g_{t,\beta}(L_{K,D})L_{K,D} - I) \| \|L_K^{r-1/2} - L_{K,D}^{r-1/2}\| \\ & \leq \left( (r/\beta)^r + ((r-1/2)/\beta)^{r-1/2} \right) t^{-r} + t^{-1/2} ((1/(2\beta))^{1/2} + 1) \\ & \quad \times \max\{1, (r-1/2)\kappa^{2r-3}\} \mathcal{R}_D^{\min\{1, r-1/2\}}. \end{aligned}$$

Plugging the above two estimates into (B12), we have

$$\mathcal{B}_{t,\beta,D} \leq C'_1 \begin{cases} \mathcal{Q}_{D,t}^{2r-1} t^{-r}, & \text{if } 1/2 \leq r \leq 1, \\ t^{-r} + t^{-1/2} \mathcal{R}_D^{\min\{1, r-1/2\}}, & \text{if } r > 1. \end{cases}$$

Then, it follows from Lemma A.3 that with confidence  $1-\delta$ , there holds  $\mathcal{Q}_{D,t}^{2r-1} \leq 2^{(2r-1)/2}$ ,  $\forall t \leq T$  and  $\mathcal{R}_D \leq \frac{4\kappa^2}{\sqrt{|D|}} \log \frac{8}{\delta}$ . This proves (28). To bound the variance, it follows from (27), (56), (48) and Lemma A.1 that

$$\begin{aligned} \mathcal{V}_{t,\beta,D} & \leq 2 \| (L_{K,D} + t^{-1}I)^{1/2} g_{t,\beta}(L_{K,D}) (L_{K,D} f_\rho - S_{D,t}^\top y_D) \|_K \\ & \leq 2 \| g_{t,\beta}(L_{K,D}) (L_{K,D} + t^{-1}I) \| \mathcal{Q}_{D,t} \mathcal{P}_{D,t} \\ & \leq 2(1+\beta) \mathcal{Q}_{D,t} \mathcal{P}_{D,t}. \end{aligned}$$

Then it follows from Lemma A.3 and Lemma A.4 that with confidence  $1-\delta$ , there holds

$$\mathcal{V}_{t,\beta,D} \leq 2\sqrt{2}(\kappa M + \gamma)(1+\beta) \mathcal{A}_{D,\lambda} \log \frac{8}{\delta} \leq 2(1+\beta) \mathcal{W}_{D,t} \log^2 \frac{16}{\delta}.$$

This completes the proof of Proposition 2.  $\blacksquare$

To prove Corollary 3, we need the following lemma derived in (Zhang et al., 2015).

**Lemma B.1** *If there exists  $L \in \mathbb{N}$  such that  $\sigma_\ell = 0$  for all  $\ell \geq L$ , then for any  $t \in \mathbb{N}$ , there holds  $\mathcal{N}(t^{-1}) \leq L$ . If there exists an  $s \in (0, 1]$  such that  $\sigma_\ell \leq \ell^{-1/s}$ , then  $\mathcal{N}(t^{-1}) \leq C_0 t^s$  for some absolute constant  $C_0 > 0$ . If there exists  $c_1, c_2 \geq 0$  such that  $\sigma_\ell \leq c_1 e^{-c_2 \ell^2}$  for all  $\ell = 1, 2, \dots$ , then  $\mathcal{N}(t^{-1}) \leq C_1 \sqrt{\log t}$ .*

We then use the above lemma and Proposition 2 to prove Corollary 3.

**Proof** [Proof of Corollary 3] Combining Lemma B.1 with (30), we get for any  $t = 1, \dots, T$

$$\mathcal{A}_{D,t} \leq \begin{cases} \frac{2\sqrt{L}}{\sqrt{|D|}}, & \text{if } \sigma_\ell = 0, \ell \geq L+1, \\ \frac{C_0 t^{s/2}}{\sqrt{|D|}}, & \text{if } \sigma_\ell \leq c_0 \ell^{-1/s}, \\ \frac{C_1 \log^{1/4} |D|}{\sqrt{|D|}}, & \text{if } \sigma_\ell \leq c_1 e^{-c_2 \ell^2}. \end{cases} \quad (\text{B14})$$

Therefore, we get from Lemma 1 and Proposition 2 that

$$\mathcal{V}_{t,\beta,D} \leq C'_1 \log \frac{8}{\delta} \begin{cases} \frac{\sqrt{L}}{\sqrt{|D|}}, & \text{if } \sigma_\ell = 0, \ell \geq L+1, \\ \frac{t^{s/2}}{\sqrt{|D|}}, & \text{if } \sigma_\ell \leq c_0 \ell^{-1/s}, \\ \frac{\log^{1/4} |D|}{\sqrt{|D|}}, & \text{if } \sigma_\ell \leq c_1 e^{-c_2 \ell^2}, \end{cases}$$

where  $C'_1 := 2\sqrt{2}(\kappa M + \gamma)(1 + \beta) \max\{2, C_0, C_1\}$ . We obtain from (28) and (31) that

$$\mathcal{B}_{t,\beta,D} \leq C'_2 \log^2 \frac{16}{\delta} \begin{cases} (|D|/L)^{-1/2}, & \text{if } \sigma_\ell = 0, \ell \geq L+1, \\ |D|^{-r/(2r+s)}, & \text{if } \sigma_\ell \leq c_0 \ell^{-1/s}, \\ (|D|/\sqrt{\log |D|})^{-1/2}, & \text{if } \sigma_\ell \leq c_1 e^{-c_2 \ell^2}, \end{cases}$$

where  $C'_2 := \max\{2^{r-1/2}, 1+4\kappa^2\}$ . Combining the above two estimates, we get from Lemma 1 and (31) that (32) holds with confidence  $1 - \delta$  and  $\tilde{C} := C'_1 + C'_2$ . This completes the proof of Corollary 3.  $\blacksquare$

**Proof** [Proof of Proposition 4] Due to (A2) and (A3), we have

$$\begin{aligned} & \|f_{t+1,\beta,D} - f_{t,\beta,D}\|_D + t^{-1/2} \|f_{t+1,\beta,D} - f_{t,\beta,D}\|_K \\ & \leq 2\beta \|(L_{K,D} + t^{-1}I)^{1/2} (L_{K,D} g_{t,\beta}(L_{K,D}) - I) S_D^\top y_D\|_K \\ & \leq 2\beta \|(L_{K,D} + t^{-1}I)^{1/2} (L_{K,D} g_{t,\beta}(L_{K,D}) - I) (L_{K,D} f_\rho - S_D^\top y_D)\|_K \\ & \quad + 2\beta \|(L_{K,D} + t^{-1}I)^{1/2} (L_{K,D} g_{t,\beta}(L_{K,D}) - I) L_{K,D} f_\rho\|_K. \end{aligned} \quad (\text{B15})$$

But (A6) yields

$$\begin{aligned} & \|(L_{K,D} + t^{-1}I)^{1/2} (L_{K,D} g_{t,\beta}(L_{K,D}) - I) (L_{K,D} f_\rho - S_D^\top y_D)\|_K \\ & \leq \mathcal{P}_{D,t} \mathcal{Q}_{D,t} \|(L_{K,D} + t^{-1}I) (L_{K,D} g_{t,\beta}(L_{K,D}) - I)\| \\ & \leq \mathcal{P}_{D,t} \mathcal{Q}_{D,t} (\|L_{K,D} (L_{K,D} g_{t,\beta}(L_{K,D}) - I)\| + t^{-1} \|(L_{K,D} g_{t,\beta}(L_{K,D}) - I)\|) \\ & \leq (1+1/\beta) t^{-1} \mathcal{P}_{D,t} \mathcal{Q}_{D,t}. \end{aligned} \quad (\text{B16})$$

If (16) holds with  $\frac{1}{2} \leq r \leq 1$ , then it follows from (A6) and (B12) that

$$\begin{aligned}
 & \| (L_{K,D} + t^{-1}I)^{1/2} (L_{K,D}g_{t,\beta}(L_{K,D}) - I) L_{K,D}f_\rho \|_K \\
 \leq & \| (L_{K,D} + t^{-1}I)^{1/2} L_{K,D} (L_{K,D}g_{t,\beta}(L_{K,D}) - I) L_K^{r-1/2} \| \|h_\rho\|_\rho \\
 \leq & \|h_\rho\|_\rho \mathcal{Q}_{D,t}^{2r-1} \|L_{K,D} (L_{K,D}g_{t,\beta}(L_{K,D}) - I) (L_{K,D} + t^{-1}I)^r \| \\
 \leq & 2^r \|h_\rho\|_\rho \mathcal{Q}_{D,t}^{2r-1} \left( \|L_{K,D}^{r+1} (L_{K,D}g_{t,\beta}(L_{K,D}) - I)\| + t^{-r} \|L_{K,D} (L_{K,D}g_{t,\beta}(L_{K,D}) - I)\| \right) \\
 \leq & 2^r \|h_\rho\|_\rho \mathcal{Q}_{D,t}^{2r-1} \left( \left( \frac{r+1}{\beta} \right)^{r+1} + \frac{1}{\beta} \right) t^{-r-1}. \tag{B17}
 \end{aligned}$$

If (16) holds with  $r > 1$ , then it follows from (A6), (B13) and (25) that

$$\begin{aligned}
 & \| (L_{K,D} + t^{-1}I)^{1/2} (L_{K,D}g_{t,\beta}(L_{K,D}) - I) L_{K,D}f_\rho \|_K \\
 \leq & \| (L_{K,D} + t^{-1}I)^{1/2} L_{K,D} (L_{K,D}g_{t,\beta}(L_{K,D}) - I) L_K^{r-1/2} \| \|h_\rho\|_\rho \\
 \leq & \| (L_{K,D} + t^{-1}I)^{1/2} L_{K,D} (L_{K,D}g_{t,\beta}(L_{K,D}) - I) L_{K,D}^{r-1/2} \| \|h_\rho\|_\rho \\
 & + \| (L_{K,D} + t^{-1}I)^{1/2} L_{K,D} (L_{K,D}g_{t,\beta}(L_{K,D}) - I) \times (L_K^{r-1/2} - L_{K,D}^{r-1/2}) \| \|h_\rho\|_\rho \\
 \leq & \|h_\rho\|_\rho \left[ \left( \frac{r+1}{\beta} \right)^{r+1} + \left( \frac{r+1/2}{\beta} \right)^{r+1/2} \right] t^{-r-1} \\
 & + \| (L_{K,D} + t^{-1}I)^{1/2} L_{K,D} (L_{K,D}g_{t,\beta}(L_{K,D}) - I) \| \|L_K^{r-1/2} - L_{K,D}^{r-1/2}\|_{HS} \|h_\rho\|_\rho \\
 \leq & \|h_\rho\|_\rho \left[ \left( \frac{r+1}{\beta} \right)^{r+1} + \left( \frac{r+1/2}{\beta} \right)^{r+1/2} \right] t^{-r-1} \\
 & + \max\{(r-1/2)\kappa^{2r-3}, 1\} \left[ \left( \frac{3}{2\beta} \right)^{3/2} + \frac{1}{\beta} \right] t^{-3/2} \mathcal{R}_D^{\min\{1, r-1/2\}}. \tag{B18}
 \end{aligned}$$

Plugging (B18), (B17) and (B16) into (B15), we obtain

$$\begin{aligned}
 & \|f_{t+1,\beta,D} - f_{t,\beta,D}\|_D \leq (2+2\beta)t^{-1} \mathcal{P}_{D,t} \mathcal{Q}_{D,t} \\
 & + c_1 \begin{cases} \mathcal{Q}_{D,t}^{2r-1} t^{-r-1}, & \text{if } \frac{1}{2} \leq r \leq 1, \\ t^{-r-1} + t^{-3/2} \mathcal{R}_D^{\min\{1, r-1/2\}}, & \text{if } r > 1. \end{cases} \tag{B19}
 \end{aligned}$$

If, in addition, (15) holds and  $t \leq T$ , then Lemmas A.3 and A.4 yield directly that (33) holds with confidence  $1 - \delta$ . This completes the proof of Proposition 4.  $\blacksquare$

**Proof** [Proof of Proposition 5] It follows from Proposition 4 that

$$\mathcal{W}_{D,\hat{t}} \leq C'_2 \begin{cases} 2^{r-1/2} \hat{t}^{-r}, & \text{if } \frac{1}{2} \leq r \leq 1, \\ \hat{t}^{-r} + 4\kappa^2 \hat{t}^{-1/2} |D|^{-\min\{1/2, r/2-1/4\}}, & \text{if } r > 1. \end{cases}$$

Therefore, we have from (35) that  $\hat{t} \leq t^*$ . Then it follows from Lemma B.1 and Lemma A.2 that for any  $t \leq T$ , with confidence  $1 - \delta$ , there holds

$$\begin{aligned}
 & \frac{\sqrt{t}}{|D|} + \frac{\sqrt{\max\{\mathcal{N}_D(t^{-1}), 1\}} (1 + 8\sqrt{t/|D|})}{\sqrt{|D|}} \\
 \leq & \left( \frac{\sqrt{t}}{|D|} + \frac{(1 + 4(1 + t/|D|))h(t)(1 + 8\sqrt{t/|D|})}{\sqrt{|D|}} \right) \log^2 \frac{16}{\delta},
 \end{aligned}$$

where

$$h(t) := \begin{cases} \sqrt{L}, & \text{if } \sigma_\ell = 0, \ell \geq L + 1, \\ C_0 t^{s/2}, & \text{if } \sigma_\ell \leq c_0 \ell^{-1/s}, \\ \sqrt{C_1} \log^{1/4} t, & \text{if } \sigma_\ell \leq c_1 e^{-c_2 \ell^2}. \end{cases} \quad (\text{B20})$$

Then, (6) yields that with confidence  $1 - \delta$ , there holds

$$\mathcal{W}_{D,t} \leq c'_2 \left( \frac{\sqrt{t}}{|D|} + \frac{81h(t)}{\sqrt{|D|}} \right) \log^2 \frac{16}{\delta} =: \mathcal{T}_{D,t,\delta}.$$

where  $c'_2 := 4\sqrt{2}(\kappa M + \gamma)$ . Define  $t^{**} := t_{D,\beta}^{**}$  as the largest integer satisfying

$$\mathcal{T}_{D,t,\delta} \leq C'_2 \begin{cases} 2^{r-1/2} t^{-r}, & \text{if } \frac{1}{2} \leq r \leq 1, \\ t^{-r} + 4\kappa^2 t^{-1/2} |D|^{-\min\{1/2, r/2-1/4\}}, & \text{if } r > 1. \end{cases} \quad (\text{B21})$$

Then, it follows from (35) that

$$t^{**} \leq t^*.$$

It is obvious that  $\mathcal{T}_{D,t,\delta}$  is non-decreasing with respect to  $t$  but the right-hand side of (B21) is non-increasing with  $t$ . Therefore, for any  $t \leq t^{**}$ , (B21) holds. Setting

$$t_0 = c_\delta \begin{cases} (|D|/L)^{\frac{1}{2r}}, & \text{if } \sigma_\ell = 0, \ell \geq L + 1, \\ |D|^{\frac{1}{2r+s}}, & \text{if } \sigma_\ell \leq c_0 \ell^{-1/s}, \\ (|D|/\sqrt{\log |D|})^{\frac{1}{2r}}, & \text{if } \sigma_\ell \leq c_1 e^{-c_2 \ell^2}, \end{cases}$$

with  $0 < c_\delta \leq 1$  depending on  $\delta$  that will be determined below, we have

$$\mathcal{T}_{D,t_0,\delta} \leq c'_2 H(|D|) \log^2 \frac{16}{\delta}$$

and

$$c'_3 c_\delta^{-r} H(|D|) \leq \begin{cases} 2^{r-1/2} t_0^{-r}, & \text{if } \frac{1}{2} \leq r \leq 1, \\ t_0^{-r} + 4\kappa^2 t_0^{-1/2} |D|^{-\min\{1/2, r/2-1/4\}}, & \text{if } r > 1, \end{cases}$$

where

$$H(|D|) := \begin{cases} (|D|/L)^{-1/2}, & \text{if } \sigma_\ell = 0, \ell \geq L + 1, \\ |D|^{-r/(2r+s)}, & \text{if } \sigma_\ell \leq c_0 \ell^{-1/s}, \\ (|D|/\sqrt{\log |D|})^{-1/2}, & \text{if } \sigma_\ell \leq c_1 e^{-c_2 \ell^2}, \end{cases} \quad (\text{B22})$$

$c'_2$  and  $c'_3$  are constants depending only on  $c'_1$ ,  $\kappa$  and  $c_0, c_1, c_2$ . It is easy to derive that there exists  $c_\delta$  such that (B21) holds. Taking  $\sigma_\ell \leq c_0 \ell^{-1/2}$  for example, if we set

$$c_\delta = \min\{1, c'_3/c'_2\}^{\frac{2}{2r+s}} \left( \log \frac{16}{\delta} \right)^{-\frac{4}{2r+s}} \leq 1,$$

then

$$c'_2 |D|^{-\frac{r}{2r+s}} c_\delta^{s/2} \log^2 \frac{16}{\delta} \leq c'_3 c_\delta^{-r} |D|^{-\frac{r}{2r+s}},$$

which implies that (B21) holds for  $t_0$ . The other two cases can be derived similarly. We remove the detailed proof for the sake of brevity. Therefore, we have  $t^* \geq t^{**} \geq t_0$ . This

proves (38). Then, it follows from Proposition 2, Lemma 1, the definition of  $t^*$  and (38) that

$$\begin{aligned}
 & \max\{\|f_{D,t^*} - f_\rho\|_\rho, \|f_{D,t^*} - f_\rho\|_D, (t^*)^{1/2}\|f_{D,t^*} - f_\rho\|_K\} \\
 & \leq 2(1 + \beta)\mathcal{W}_{D,t^*} \log^2 \frac{16}{\delta} \\
 & + C'_1 \log^2 \frac{16}{\delta} \begin{cases} 2^{r-1/2}t^{-r}, & \text{if } \frac{1}{2} \leq r \leq 1, \\ (t^*)^{-r+4\kappa^2(t^*)^{-1/2}}|D|^{-\min\{1/2, r/2-1/4\}}, & \text{if } r > 1 \end{cases} \\
 & \leq C'_3 \log^2 \frac{16}{\delta} \begin{cases} 2^{r-1/2}t_0^{-r}, & \text{if } \frac{1}{2} \leq r \leq 1, \\ t_0^{-r+4\kappa^2t_0^{-1/2}}|D|^{-\min\{1/2, r/2-1/4\}}, & \text{if } r > 1 \end{cases} \\
 & \leq \tilde{C}' \log^2 \frac{16}{\delta} \begin{cases} (|D|/L)^{-1/2}, & \text{if } \sigma_\ell = 0, \ell \geq L + 1, \\ |D|^{-r/(2r+s)}, & \text{if } \sigma_\ell \leq c_0\ell^{-1/s}, \\ (|D|/\sqrt{\log |D|})^{-1/2}, & \text{if } \sigma_\ell \leq c_1e^{-c_2\ell^2}, \end{cases}
 \end{aligned}$$

where  $C'_3$  and  $\tilde{C}'$  are constants independent of  $\delta, |D|$  or  $t$ . This completes the proof of Proposition 5.  $\blacksquare$

### Appendix C: Proof of Theorem 6

With the help of Proposition 2, Proposition 4 and Proposition 5, we can prove Theorem 6 as follows.

**Proof** [Proof of Theorem 6] We divide the proof into two cases: 1)  $\hat{t} < t_0$ ; 2)  $\hat{t} \geq t_0$ , where  $t_0$  is specified in (37). For the first case, i.e.,  $\hat{t} < t_0$ , it follows from the triangle inequality that

$$\|f_{\hat{t},\beta,D} - f_\rho\|_* \leq \|f_{\hat{t},\beta,D} - f_{t_0,\beta,D}\|_* + \|f_{t_0,\beta,D} - f_\rho\|_*, \quad (\text{C23})$$

where  $\|\cdot\|_*$  denotes either  $\|\cdot\|_\rho, t_0^{-1/2}\|\cdot\|_K$  or  $\|\cdot\|_D$ . But Corollary 3 shows that

$$\begin{aligned}
 & \max(\|f_{t_0,\beta,D} - f_\rho\|_\rho, \|f_{t_0,\beta,D} - f_\rho\|_D, t_0^{-\frac{1}{2}}\|f_{t_0,\beta,D} - f_\rho\|_K) \\
 & \leq \tilde{C} \log^2 \frac{16}{\delta} \begin{cases} (|D|/L)^{-1/2}, & \text{if } \sigma_\ell = 0, \ell \geq L + 1, \\ |D|^{-r/(2r+s)}, & \text{if } \sigma_\ell \leq c_0\ell^{-1/s}, \\ (|D|/\sqrt{\log |D|})^{-1/2}, & \text{if } \sigma_\ell \leq c_1e^{-c_2\ell^2}, \end{cases} \quad (\text{C24})
 \end{aligned}$$

holds with confidence  $1 - \delta$ . Therefore, it suffices to bound  $\|f_{\hat{t},\beta,D} - f_{t_0,\beta,D}\|_\rho$ . From the triangle inequality again, we get

$$\|f_{\hat{t},\beta,D} - f_{t_0,\beta,D}\|_* \leq \sum_{k=\hat{t}}^{t_0-1} \|f_{k+1,\beta,D} - f_{k,\beta,D}\|_*.$$

For an arbitrary  $k = \hat{t}, \dots, t_0 - 1$ , Lemma 1 shows that with confidence  $1 - \delta$ , there holds

$$\|f_{k+1,\beta,D} - f_{k,\beta,D}\|_* \leq 2(1 + \beta)\bar{c}_1 k^{-1} \mathcal{W}_{D,k} \log^4 \frac{16}{\delta}.$$

Since Lemma B.1 and Lemma A.2 yield that with confidence  $1 - \delta$ ,

$$\begin{aligned} & \frac{\sqrt{t}}{|D|} + \frac{\sqrt{\max\{\mathcal{N}_D(t^{-1}), 1\}}(1 + 8\sqrt{t/|D|})}{\sqrt{|D|}} \\ & \leq \left( \frac{\sqrt{t}}{|D|} + \frac{(1 + 4(1 + t/|D|))h(t)(1 + 8\sqrt{t/|D|})}{\sqrt{|D|}} \right) \log^2 \frac{16}{\delta}, \end{aligned}$$

where  $h(t)$  is given by (B20), then, (6) implies that with confidence  $1 - \delta$ , there holds

$$\mathcal{W}_{D,t} \leq c'_4 \left( \frac{\sqrt{t}}{|D|} + \frac{(1 + 4(1 + t/|D|))h(t)(1 + 8\sqrt{t/|D|})}{\sqrt{|D|}} \right) \quad (\text{C25})$$

where  $c'_4 := 4\sqrt{2}(\kappa M + \gamma)$ . Hence, for arbitrary  $k \leq t_0 \leq \tilde{c}|D|$ , with confidence  $1 - \delta$ , we get from (B20) that

$$\mathcal{W}_{D,k} \leq \bar{c}_2 \frac{h(t)}{\sqrt{|D|}} \left( 1 + \frac{k^{1/2}(h(k))^{-1}}{\sqrt{|D|}} \right) \leq 2\bar{c}_2 \frac{h(t)}{\sqrt{|D|}},$$

where  $\bar{c}_2 := c'_4(1 + \tilde{c})(\sqrt{\tilde{c} + 1} + (5 + 4\tilde{c})(C_0 + 1 + \sqrt{C_1})(1 + 8\tilde{c}))^2$ . If  $\sigma_\ell \leq c_0\ell^{-1/s}$ , then for any  $k = \hat{t}, \dots, t_0 - 1$ ,  $r \geq 1/2$  yields

$$\begin{aligned} \|f_{t_0,\beta,D} - f_{\hat{t},\beta,D}\|_* & \leq 8\bar{c}_1\bar{c}_2(1 + \beta) \log^4 \frac{16}{\delta} \sum_{k=\hat{t}}^{t_0-1} k^{-1} \frac{h(k)}{\sqrt{|D|}} \\ & \leq 8\bar{c}_1\bar{c}_2(1 + \beta)(2s + 1) \frac{t_0^{s/2}}{\sqrt{|D|}} \log^4 \frac{16}{\delta} \\ & \leq \bar{c}_3 |D|^{-r/(2r+s)} \log^4 \frac{16}{\delta}. \end{aligned}$$

where  $\bar{c}_3 := 4\bar{c}_1\bar{c}_2\tilde{c}^{s/2}(1 + \beta)(2s + 1)(1 + \tilde{c}^{(1+s)/2})$ . If  $\sigma_\ell = 0, \ell \geq L + 1$ , the same approach together with  $h(k) = L$  yields

$$\|f_{t_0,\beta,D} - f_{\hat{t},\beta,D}\|_* \leq \bar{c}_3 \frac{\sqrt{L} \log |D|}{|D|} \log^4 \frac{16}{\delta}.$$

Similar, for  $\sigma_\ell \leq c_1 e^{-c_2\ell^2}$ , we get

$$\|f_{t_0,\beta,D} - f_{\hat{t},\beta,D}\|_* \leq \bar{c}_3 \frac{\log |D|}{|D|} \log^4 \frac{16}{\delta}.$$

Plugging the above three estimates and (C24) into (C23), we get with confidence  $1 - \delta$ , there holds

$$\|f_{\hat{t},\beta,D} - f_\rho\|_* \leq \bar{c}_4 \log^4 \frac{16}{\delta} \begin{cases} \frac{\sqrt{L} \log |D|}{\sqrt{|D|}}, & \text{if } \sigma_\ell = 0, \ell \geq L + 1, \\ |D|^{-r/(2r+s)} & \text{if } \sigma_\ell \leq c_0\ell^{-1/s}, \\ \frac{\log |D|}{\sqrt{|D|}}, & \text{if } \sigma_\ell \leq c_1 e^{-c_2\ell^2} \end{cases}$$

with  $\bar{c}_4 = \bar{c}_3 + \tilde{C}$ . Now, we turn to the second case:  $\hat{t} \geq t_0$ . Under this circumstance, we get from the definitions of  $\hat{t}$ ,  $t^*$  and Proposition 5 that

$$\begin{aligned}
 & \|f_{\hat{t},\beta,D} - f_\rho\|_\rho \\
 \leq & 2(1+\beta)\mathcal{W}_{D,\hat{t}} \log^2 \frac{16}{\delta} + \log^2 \frac{16}{\delta} \begin{cases} 2^{r-1/2}\hat{t}^{-r}, & \text{if } \frac{1}{2} \leq r \leq 1, \\ \hat{t}^{-r} + 4\kappa^2\hat{t}^{-1/2}|D|^{-\min\{1/2,r/2-1/4\}}, & \text{if } r > 1 \end{cases} \\
 \leq & \bar{c}_8 \log^2 \frac{16}{\delta} \begin{cases} 2^{r-1/2}\hat{t}^{-r}, & \text{if } \frac{1}{2} \leq r \leq 1, \\ \hat{t}^{-r} + 4\kappa^2\hat{t}^{-1/2}|D|^{-\min\{1/2,r/2-1/4\}}, & \text{if } r > 1 \end{cases} \\
 \leq & \bar{c}_8 \log^2 \frac{16}{\delta} \begin{cases} 2^{r-1/2}t_0^{-r}, & \text{if } \frac{1}{2} \leq r \leq 1, \\ t_0^{-r} + 4\kappa^2t_0^{-1/2}|D|^{-\min\{1/2,r/2-1/4\}}, & \text{if } r > 1 \end{cases} \\
 \leq & \bar{c}_9 \log^2 \frac{16}{\delta} \begin{cases} (|D|/L)^{-1/2}, & \text{if } \sigma_\ell = 0, \ell \geq L+1, \\ |D|^{-r/(2r+s)} & \text{if } \sigma_\ell \leq c_0\ell^{-1/s}, \\ (|D|/\sqrt{\log|D|})^{-1/2}, & \text{if } \sigma_\ell \leq c_1e^{-c_2\ell^2}, \end{cases}
 \end{aligned}$$

where  $\bar{c}_8, \bar{c}_9$  are constants independent of  $|D|, \delta$  or  $t$ . The bound of  $\|f_{\hat{t},\beta,D} - f_\rho\|_D$  and  $\|f_{\hat{t},\beta,D} - f_\rho\|_K$  can be derived by the same method. We remove the details for the sake of brevity. This completes the proof of Theorem 6.  $\blacksquare$